EPFL Physics and Applied Physics master programs - A.Y. 2024-2025

Introduction to astroparticle physics

Part 2 – Lesson 5 – May 23, 2025

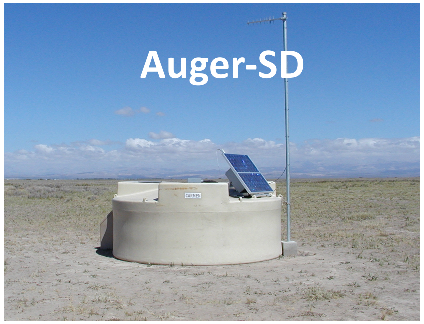

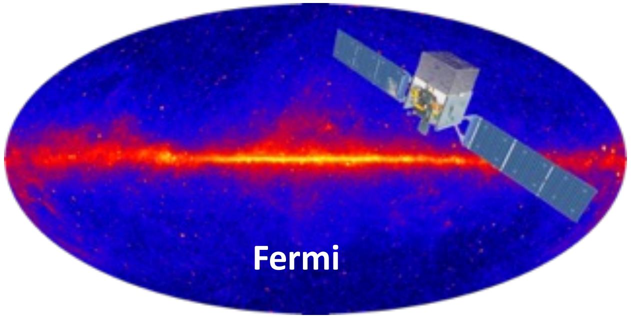

Prof. Chiara Perrina

E-mail: Chiara.Perrina@epfl.ch

Learning outcomes and goals

- Describe the cosmic ray (CR) energy spectrum and composition. Discuss CR origin, acceleration and propagation.
- Explain the relationship between charged CRs, gamma-rays and neutrinos.
- Discuss the detection principles and measured quantities (mass, charge, momentum, energy, rigidity, direction, …) of astroparticle physics experiments.
- Interpret the main results of selected experiments
- Assess / Evaluate the state of the art of astroparticle physics

PAO: Pierre Auger Observatory (2008—now)

The Auger headquarters are in Malargüe: a city in the province of Mendoza (Argentina), in the foothills of the Andes.

Map data ©2021 Google, INEGI 2000 km

Auger is a ground-based, hybrid detector, which studies the cosmic rays at the highest energies.

By observing the EASs, Auger measures the <u>energy</u>, the <u>arrival direction</u> and the <u>mass</u> of the primary cosmic rays.

Map data ©2021 Google 200 km

https://www.auger.org

PAO Collaboration (18 Countries)

1) Argentina
2) Australia
3) Belgium
4) Brazil
5) Colombia
6) Czech Republic
7) France
8) Germany
9) Italy
10) Mexico
11) Poland
12) Peru
13) Portugal
14) Romania
15) Slovenia
16) Spain
17) The Netherlands
18) USA

https://www.auger.org/collaboration/institutions

The Surface Detector (SD)

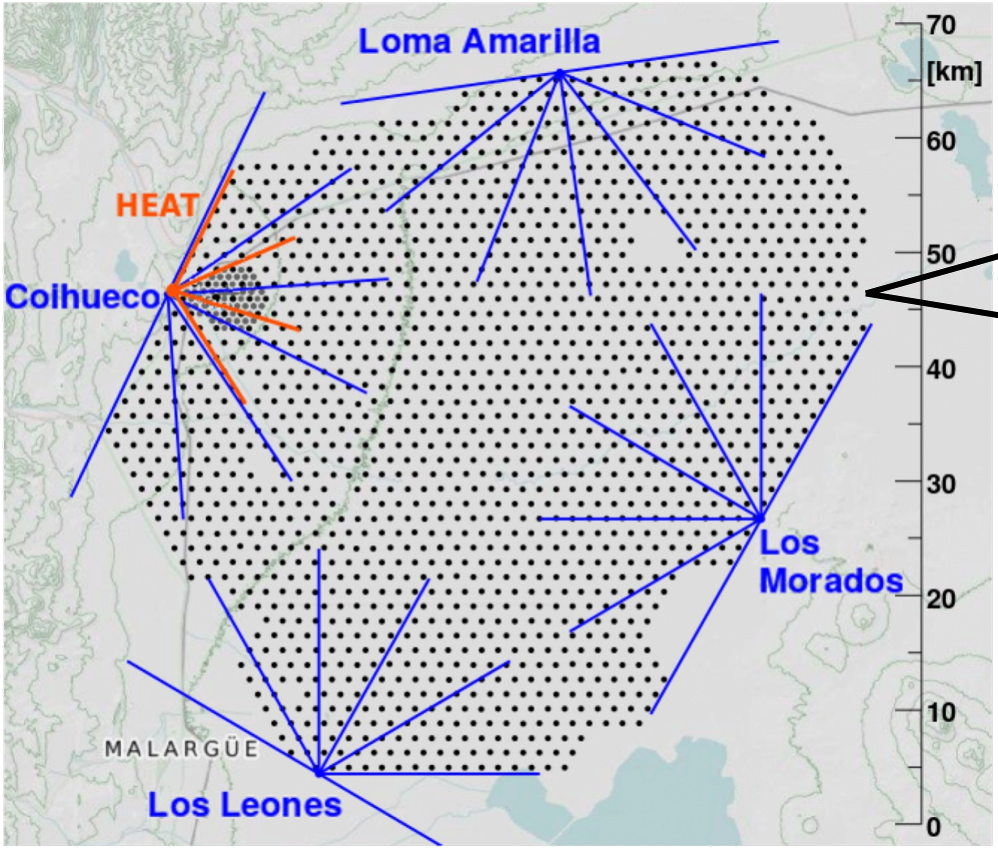

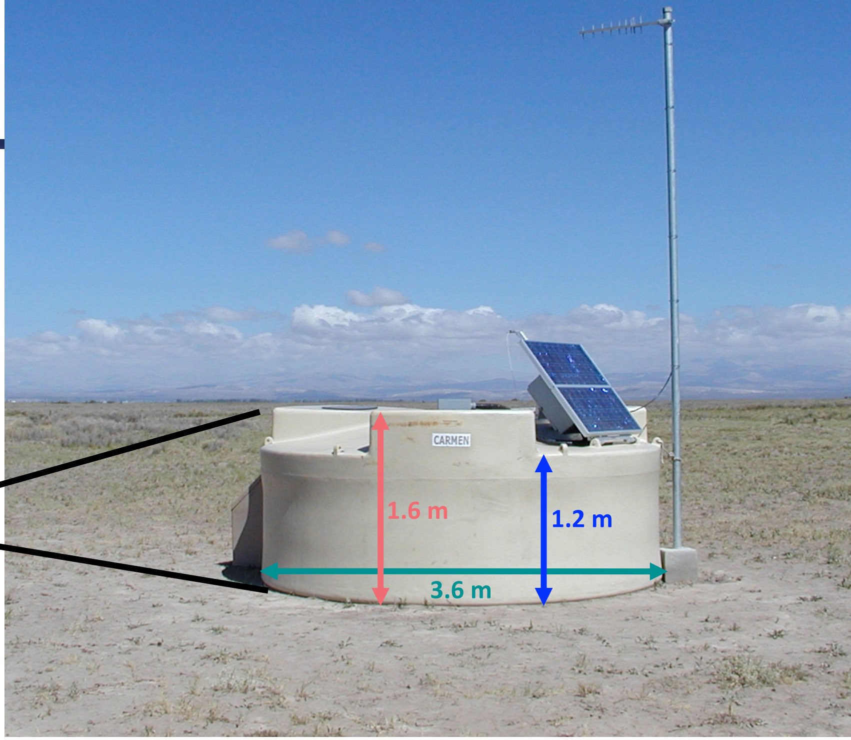

- The black dots indicate the water Cherenkov tanks.

The Surface Detector (SD) covers an area of **3’000 km^2** and consists of:

- **1’600 water Cherenkov detectors** arranged in a triangular grid with nearest neighbors separated by **1.5 km** (SD-1500 array);
- **61** water Cherenkov detectors distributed over 23.5 km^2 and separated by **750 m** (SD-750 or ‘infill’ array).

Water-Cherenkov tanks

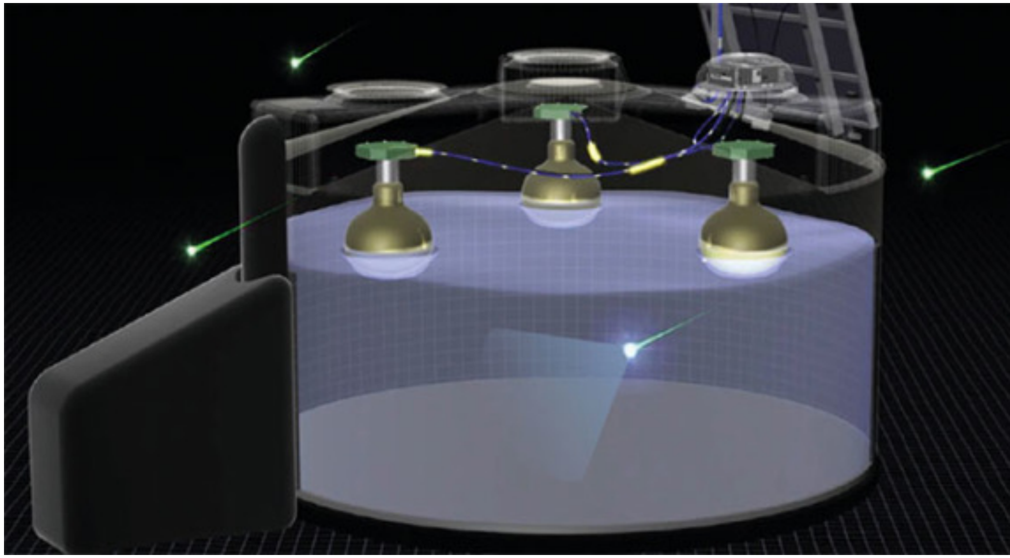

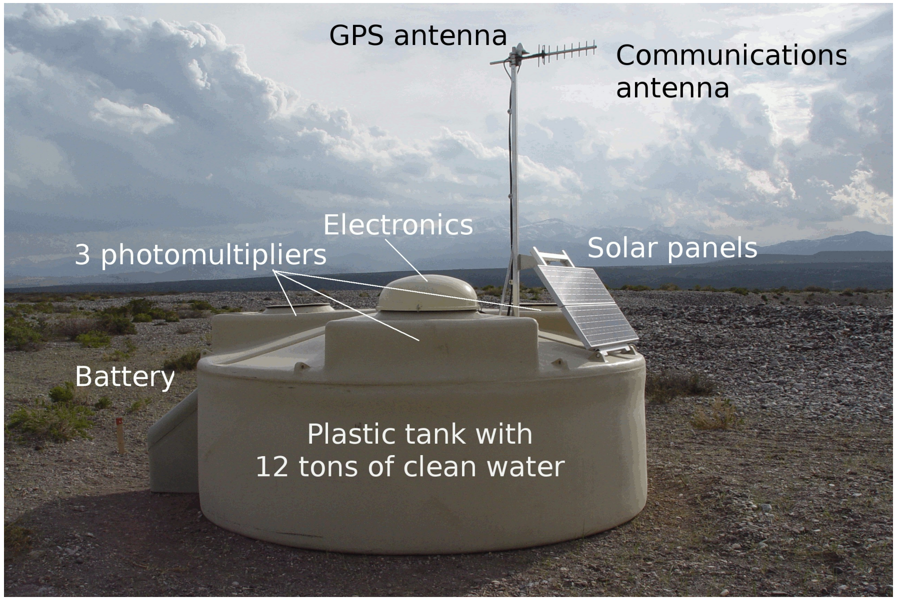

https://www.flickr.com/photos/134252569@N07/22094523800/in/album-72157659225375559/

Atmospheric fluorescence

When charged particles of an EAS interact with Nitrogen molecules in air, the Nitrogen molecules get excited. When they return to their ground state a typical radiation (5000 photons/km) **in the wavelength range between 300 nm to 450 nm is emitted.**

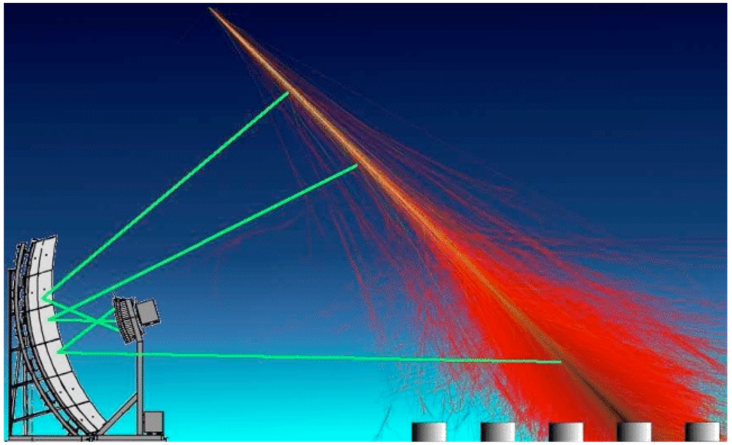

It can travel several kilometers through the atmosphere and detected by an optical telescope, i.e., mirrors and PMTs, typically equipped with fast response electronics (fluorescence detectors).

Fluorescence detectors have low duty cycles: they can collect data only during cloudless and moonless nights.

The fluorescence light is emitted **isotropically** while the Cherenkov light is **directional** emitted in a narrow cone of angle $\theta \sim 1°$, although Coulomb scattering of the electrons will considerably broaden the Cherenkov cone.

The Fluorescence Detector (FD)

https://en.wikipedia.org/wiki/Pierre_Auger_Observatory

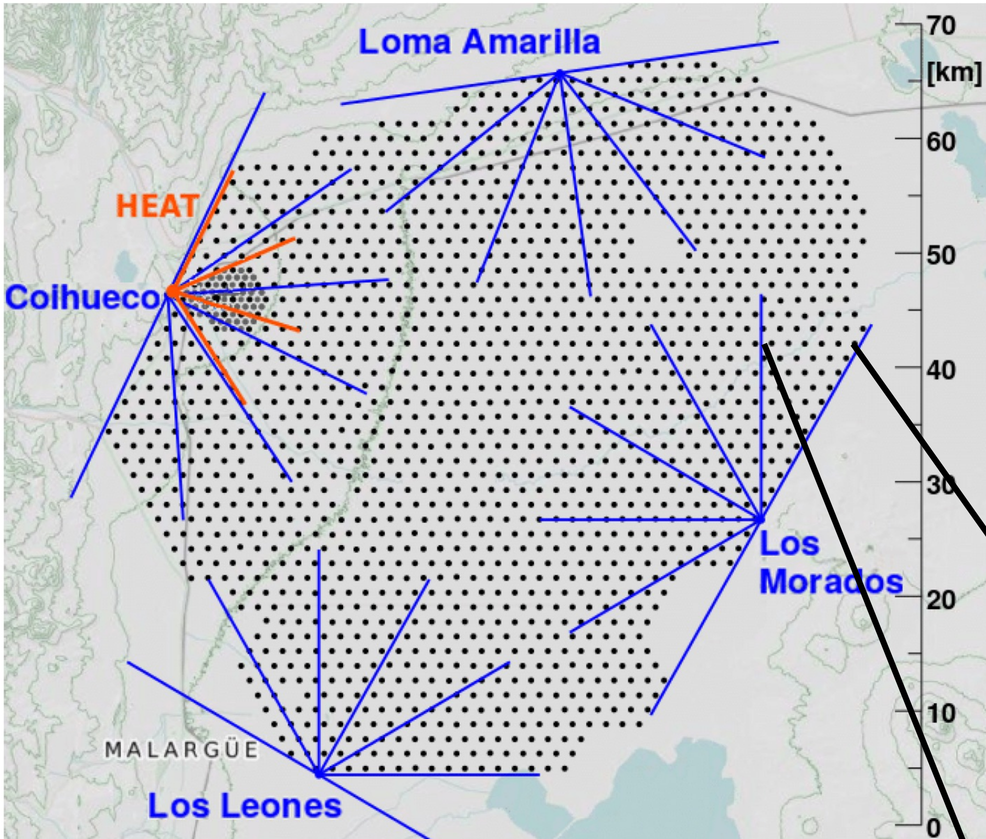

https://www.flickr.com/photos/134252569@N07/22095735509/in/album-72157659225375559/

The **Fluorescence Detector (FD)** consists of 4 telescope buildings (eyes) overlooking SD. Each building houses 6 telescopes with a 30° × 28.5° field of view. The fluorescence light is focused by a spherical mirror of ∼13 m^2 into a camera consisting of 440 PMTs.

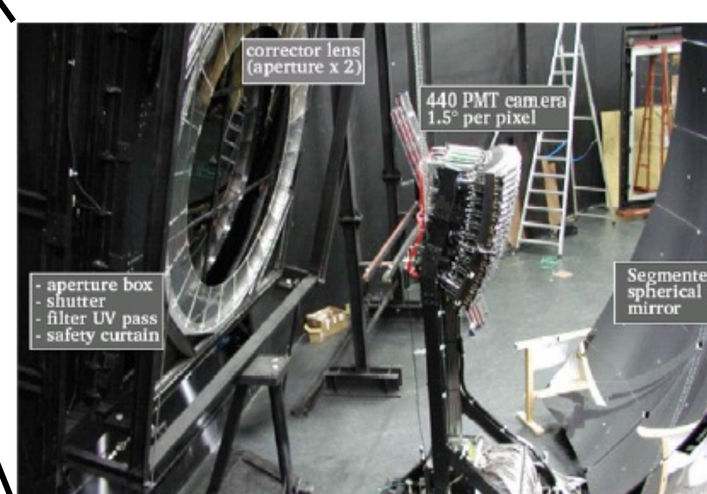

- The blue dots indicate the position of the 4 telescope buildings.
- The red dot indicates the position of the 3 HEATs: the High Elevation Auger Telescopes.

The Fluorescence Telescopes

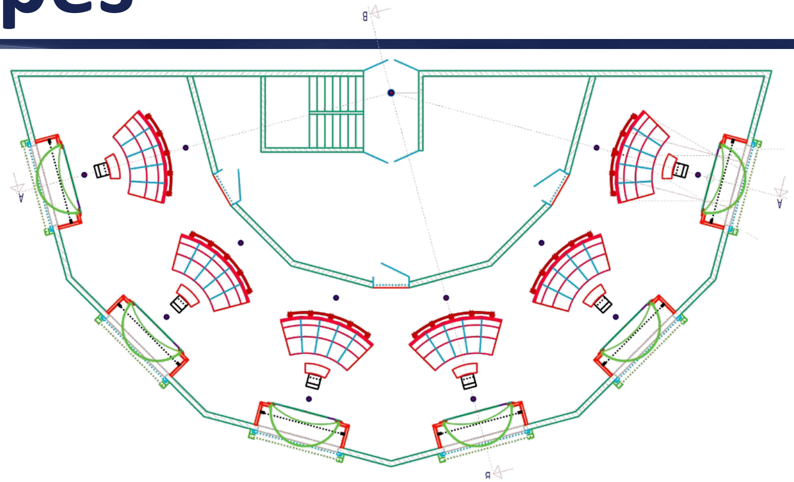

elevation $1.5° - 30°$

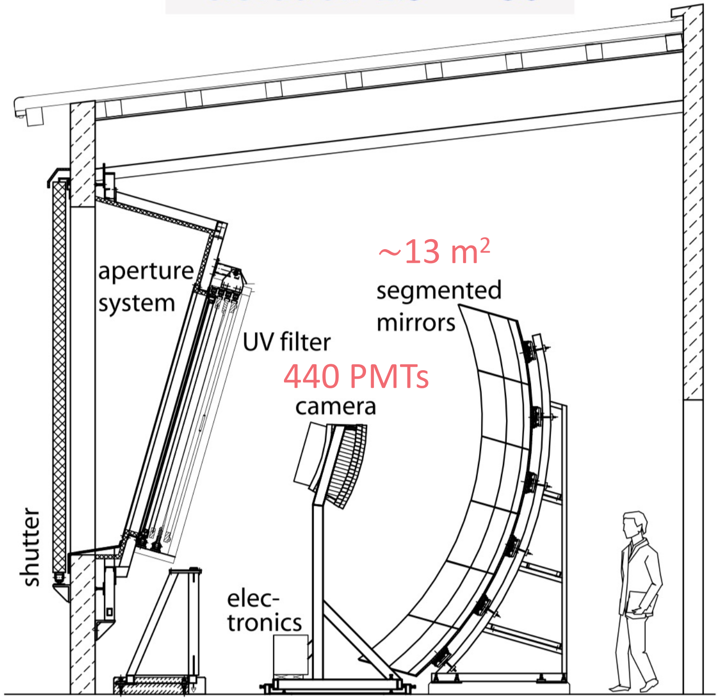

https://www.youtube.com/watch?v=dcNxkiz_hec

The High Elevation Auger Telescopes (HEAT)

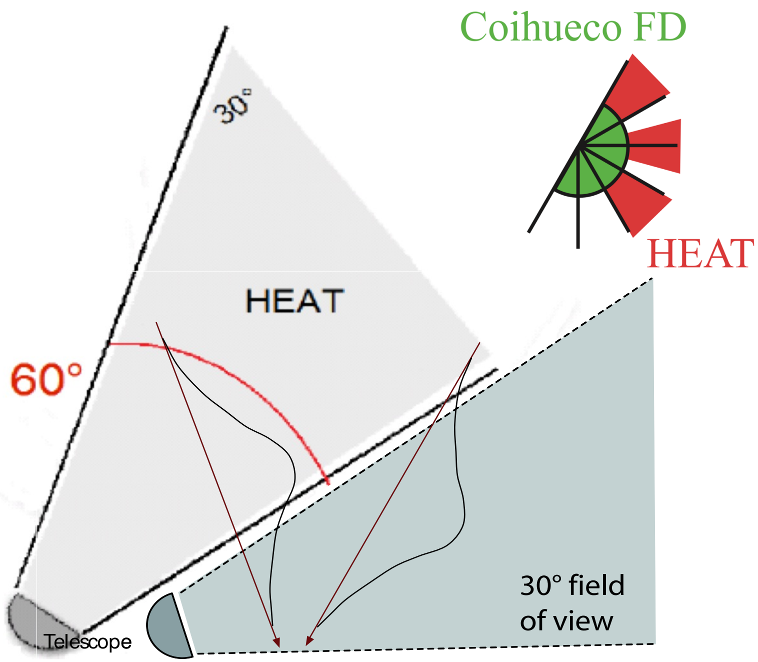

elevation $30^{\circ} - 58^{\circ}$

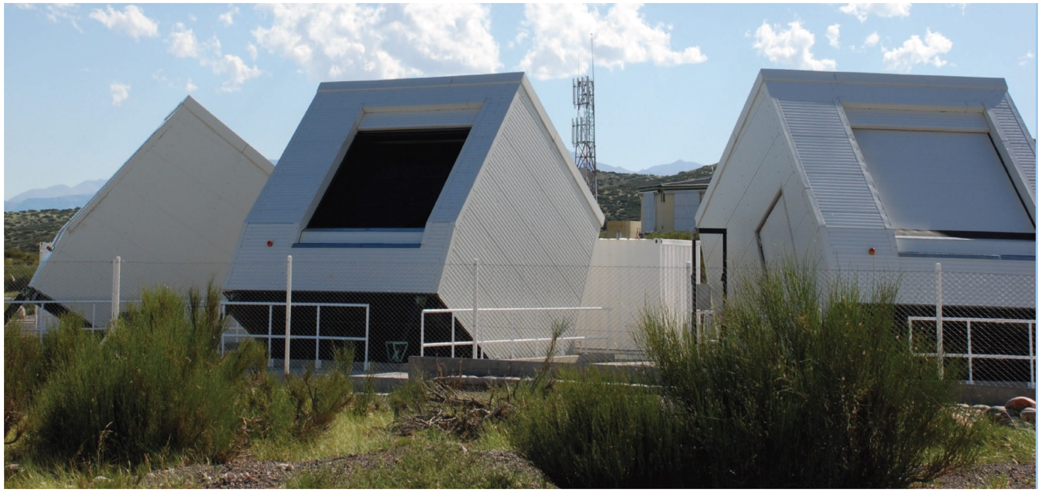

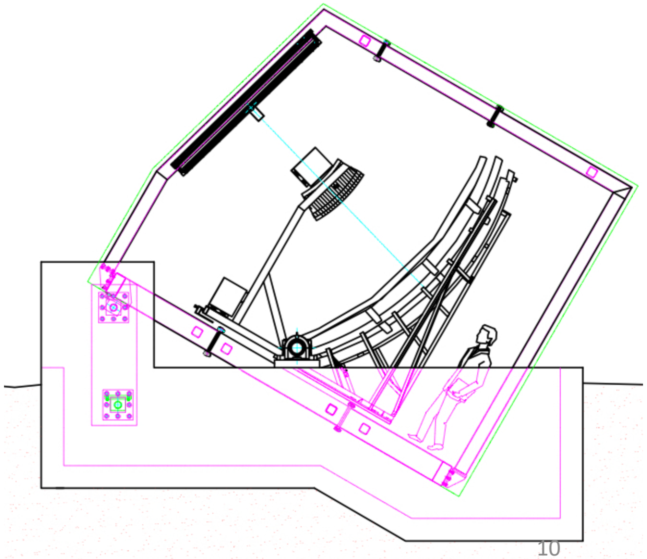

Auger: a ground-based hybrid detector

The main feature of Auger is the hybrid design → Auger can observe air showers simultaneously with two different and complementary techniques.

DUTY CYCLE

FD: 10%

SD: 100%

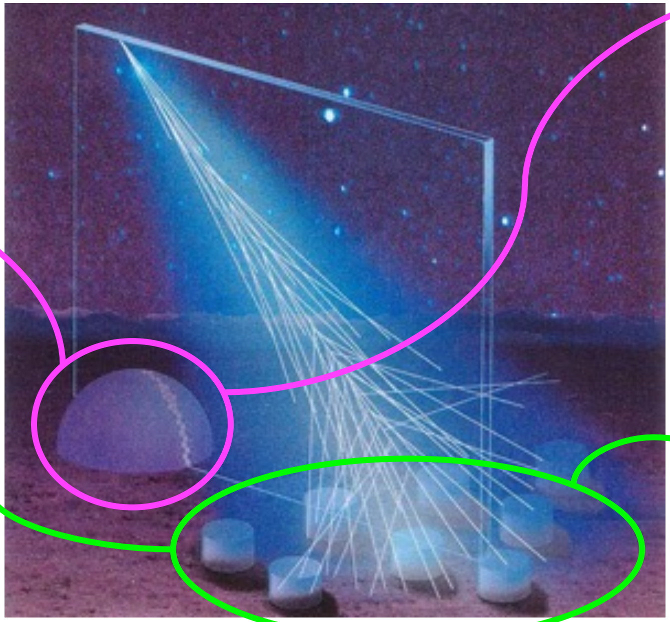

TASK

FD: measures the EAS **longitudinal profile** → energy and mass of the primary CR

SD: measures the EAS **lateral profile** → direction and energy of the primary CR

Reconstruction of the primary CR direction with the SD

When a charged particle of the EAS induces the Cherenkov effect inside the water tank, the Cherenkov light is detected by 3 photomultipliers, the analog signal is converted into a digital signal by three FADCs (one for each photomultiplier) and expressed in VEM (Vertical Equivalent Muon, response to a muon traveling vertically and centrally through a tank).

The incoming direction of the primary, or the direction of the shower axis, is determined by measuring the arrival times (T1, T2, T3, ...) of the shower front on three or more Cherenkov stations.

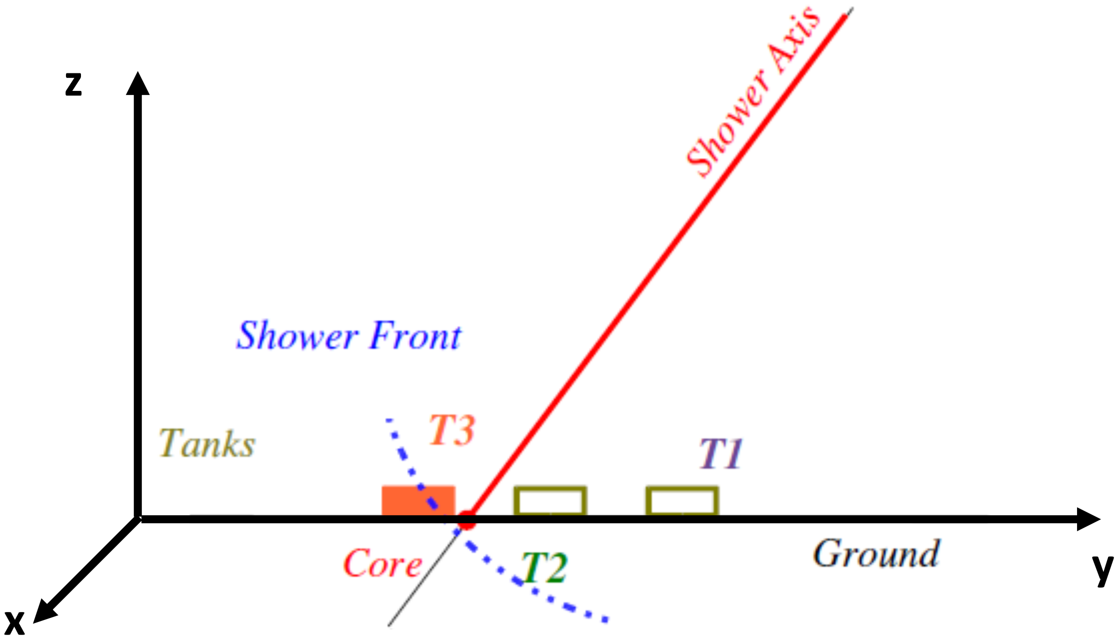

[Auger Collaboration, 2020 JINST 15 P10021](#)

Reconstruction of the primary CR direction with the SD

When a charged particle of the EAS induces the Cherenkov effect inside the water tank, the Cherenkov light is detected by 3 photomultipliers, the analog signal is converted into a digital signal by three FADCs (one for each photomultiplier) and expressed in VEM (Vertical Equivalent Muon, response to a muon traveling vertically and centrally through a tank).

The incoming direction of the primary, or the direction of the shower axis, is determined by measuring the arrival times (T1, T2, T3, ...) of the shower front on three or more Cherenkov stations.

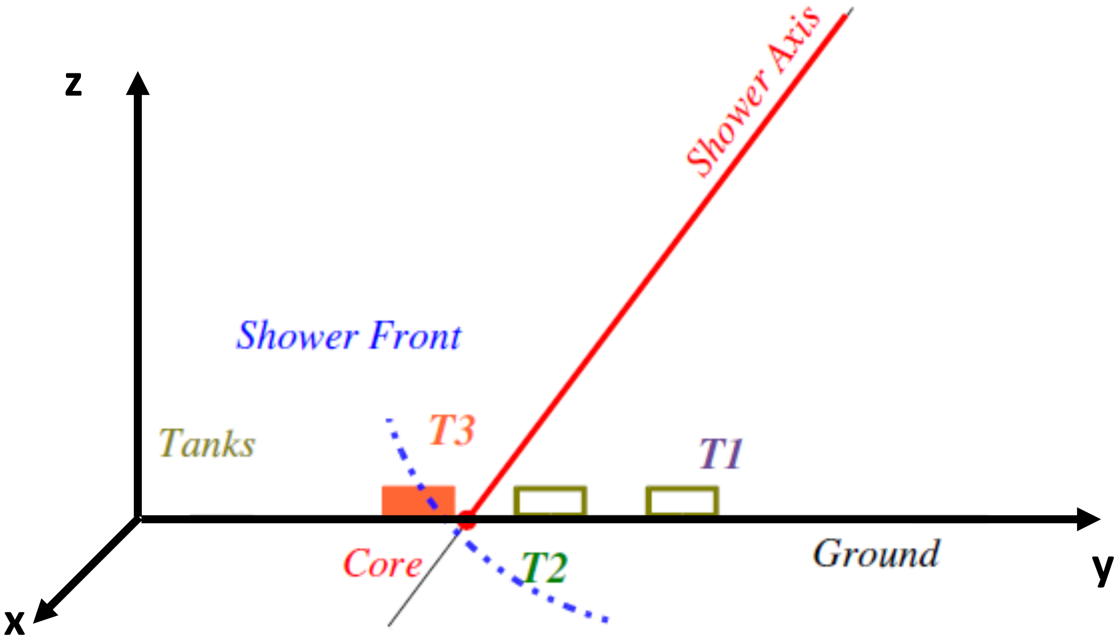

$$x_{\text{core}} = \frac{\sum_i W_i\, x_i}{\sum_i W_i}$$

$$y_{\text{core}} = \frac{\sum_i W_i\, y_i}{\sum_i W_i}$$

$$z_{\text{core}} = \frac{\sum_i W_i\, z_i}{\sum_i W_i} = 0$$

$$W_i = \sqrt{S_i}$$

Auger Collaboration, 2020 JINST 15 P10021

Reconstruction of the primary CR direction with the SD

When a charged particle of the EAS induces the Cherenkov effect inside the water tank, the Cherenkov light is detected by 3 photomultipliers, the analog signal is converted into a digital signal by three FADCs (one for each photomultiplier) and expressed in VEM (Vertical Equivalent Muon, response to a muon traveling vertically and centrally through a tank).

The incoming direction of the primary, or the direction of the shower axis, is determined by measuring the arrival times (T1, T2, T3, ...) of the shower front on three or more Cherenkov stations.

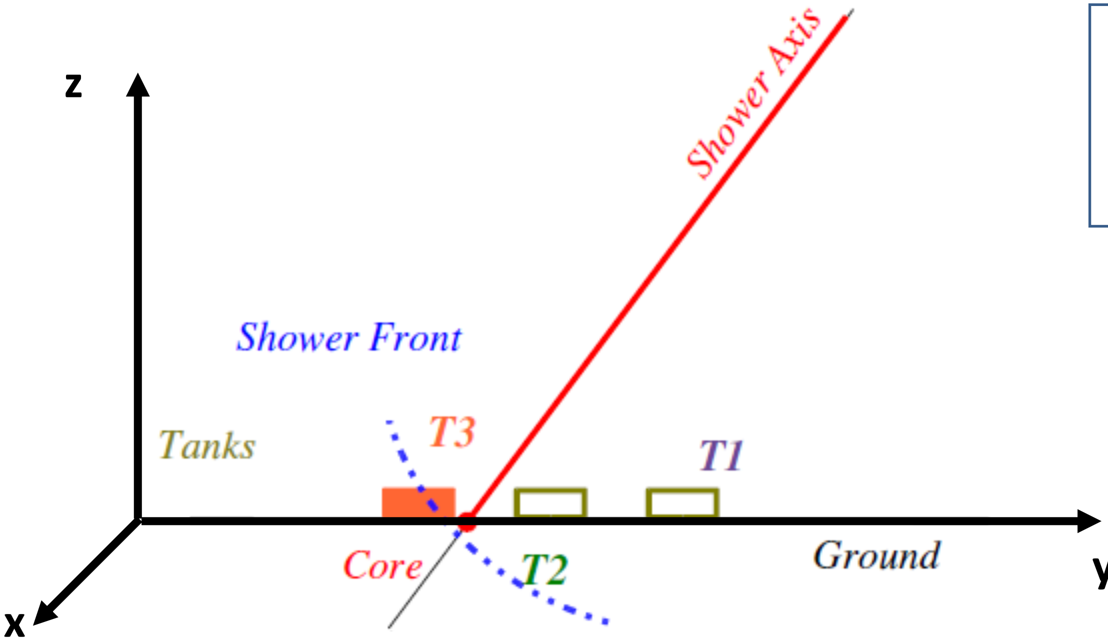

$$u\,(x - x_{\text{core}}) + v\,(y - y_{\text{core}}) = 0$$

Directional cosines: $u = \sin\theta\cos\phi$

$v = \sin\theta\sin\phi$

$$d_i = c\,t_i$$

$$d_{\text{core}} = c\,t_{\text{core}}$$

$$d_i + d_{i,\text{core}} = d_{\text{core}}$$

⇩

$$t_i = t_{\text{core}} - \frac{u\,(x_i - x_{\text{core}}) + v\,(y_i - y_{\text{core}})}{c}$$

$$\chi^2 = \sum_i \frac{(T_i - t_i)^2}{\sigma_i^2}$$

$$x_{\text{core}} = \frac{\sum_i W_i\,x_i}{\sum_i W_i}$$

$$y_{\text{core}} = \frac{\sum_i W_i\,y_i}{\sum_i W_i}$$

$$z_{\text{core}} = \frac{\sum_i W_i\,z_i}{\sum_i W_i} = 0$$

$$W_i = \sqrt{S_i}$$

Auger Collaboration, 2020 JINST 15 P10021

Reconstruction of the primary CR direction with the SD

When a charged particle of the EAS induces the Cherenkov effect inside the water tank, the Cherenkov light is detected by 3 photomultipliers, the analog signal is converted into a digital signal by three FADCs (one for each photomultiplier) and expressed in VEM (Vertical Equivalent Muon, response to a muon traveling vertically and centrally through a tank).

The incoming direction of the primary, or the direction of the shower axis, is determined by measuring the arrival times (T1, T2, T3, ...) of the shower front on three or more Cherenkov stations.

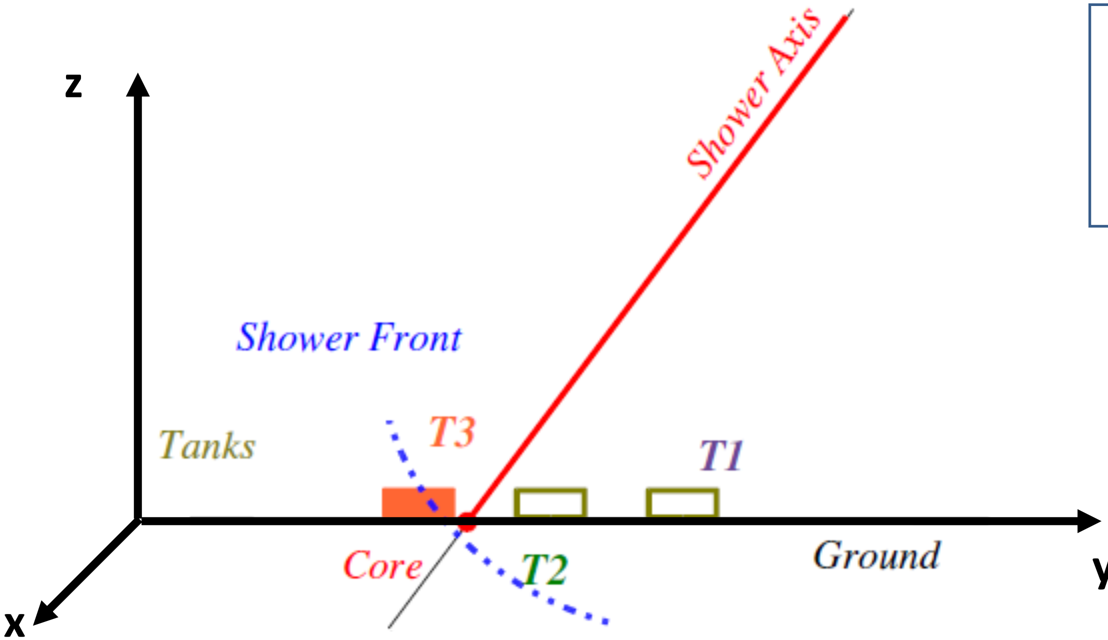

$$u\,(x - x_{\text{core}}) + v\,(y - y_{\text{core}}) = 0$$

$$u = \sin\theta\cos\phi$$

$$v = \sin\theta\sin\phi$$

$$d_i = c\,t_i$$

$$d_{\text{core}} = c\,t_{\text{core}}$$

$$d_i + d_{i,\text{core}} = d_{\text{core}}$$

$$t_i = t_{\text{core}} - \frac{u\,(x_i - x_{\text{core}}) + v\,(y_i - y_{\text{core}})}{c}$$

$$\chi^2 = \sum_i \frac{(T_i - t_i)^2}{\sigma_i^2}$$

$$x_{\text{core}} = \frac{\sum_i W_i\, x_i}{\sum_i W_i}$$

$$y_{\text{core}} = \frac{\sum_i W_i\, y_i}{\sum_i W_i}$$

$$z_{\text{core}} = \frac{\sum_i W_i\, z_i}{\sum_i W_i} = 0$$

$$W_i = \sqrt{S_i}$$

Auger Collaboration, 2020 JINST 15 P10021

Measurement of the primary CR energy with the SD

https://opendata.auger.org/display.php «Golden Hybrid event 2»

A shower detected by the SD and by the FD, reconstructed with zenith angle θ = 36.3° and energy *E* = 16.76 EeV.

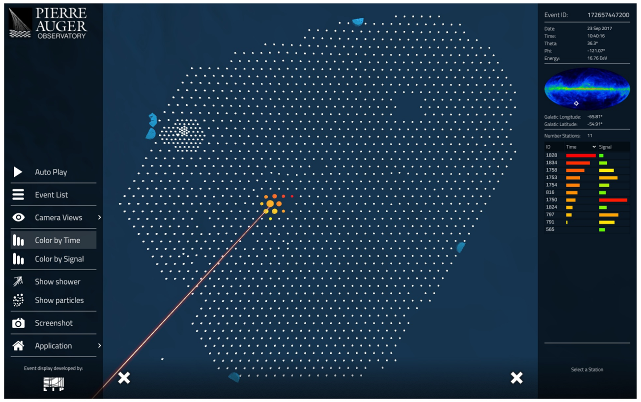

- The colored stations are the stations participating in this event.
- The color indicates the trigger time (yellow is early, red is late).
- The area of the triggered stations is proportional to the logarithm of the signal.

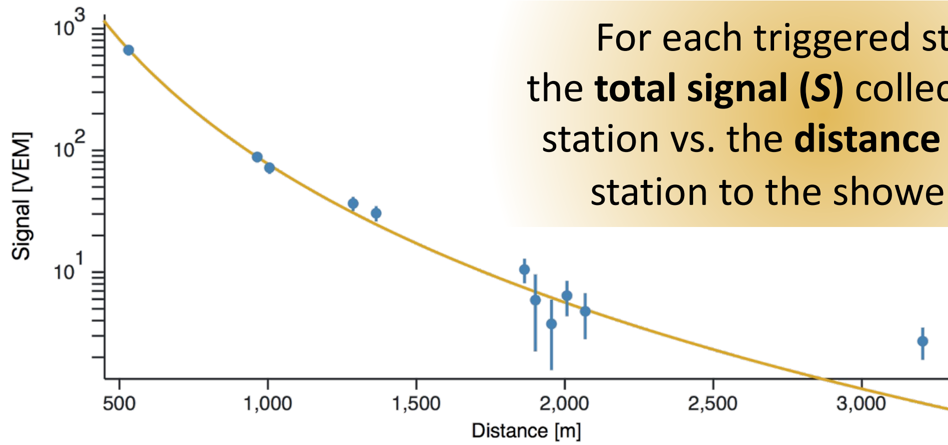

For each triggered station: the **total signal (*S*)** collected in the station vs. the **distance (*r*)** of the station to the shower core.

- The shower lateral profile is fitted with a log-log parabola (Herald method):

$$\ln(S) = A \ln r - B(\ln r)^2$$

- In 1970, Hillas discovered that the particle density at large distances from the core (400–1200 m) is proportional to the energy of the primary particle and is independent of both its nature and the interaction models. This finding has been confirmed by numerous Monte Carlo simulations.

→The signal at 1000 m from the core gives an estimate of the energy of the primary CR.

Measurement of the shower X_{max} with the FD

A shower detected by the SD and by the FD, reconstructed with zenith angle θ = 36.3° and energy *E* = 16.76 EeV.

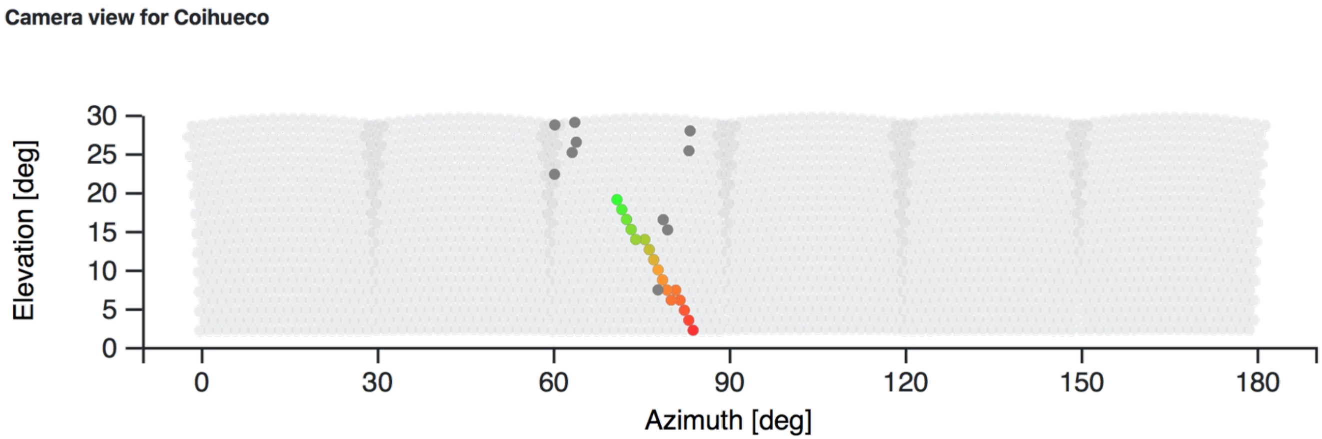

- The color indicates the time at which the light reaches each pixel (
- Dark pixels are random coincidences and are not used in the reconstruction.

Fit of the shower profile with an empirical function (Gaisser-Hillas function) → Direct measurement of X_{max} with the FD

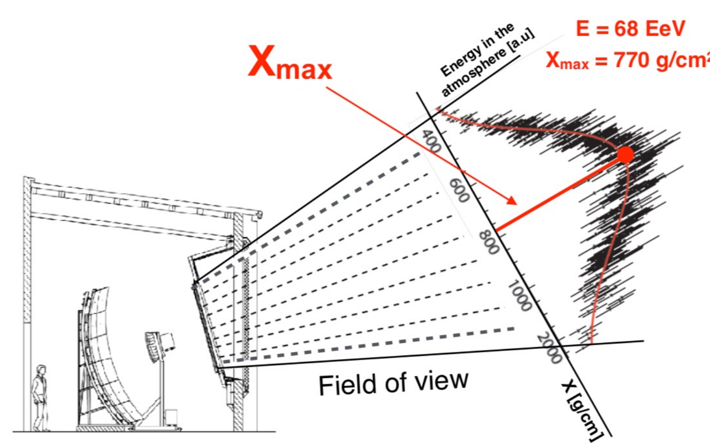

Measurement of the shower X_{max} with the FD

A shower detected by the SD and by the FD, reconstructed with zenith angle θ = 36.3° and energy *E* = 16.76 EeV.

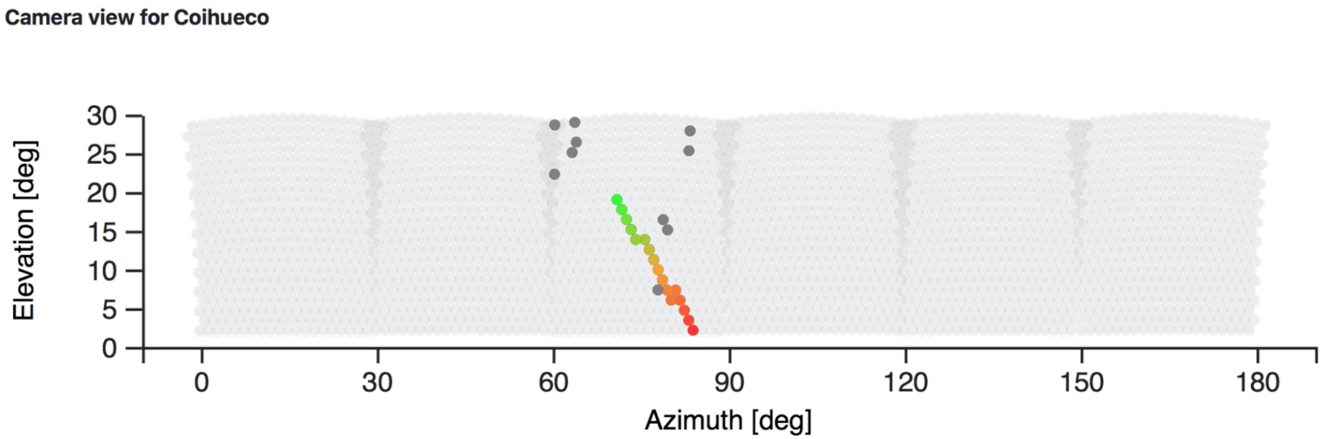

- The color indicates the time at which the light reaches each pixel (green is early, red is late).
- Dark pixels are random coincidences and are not used in the reconstruction.

Fit of the shower profile with an empirical function (Gaisser-Hillas function) → Direct measurement of X_{max} with the FD

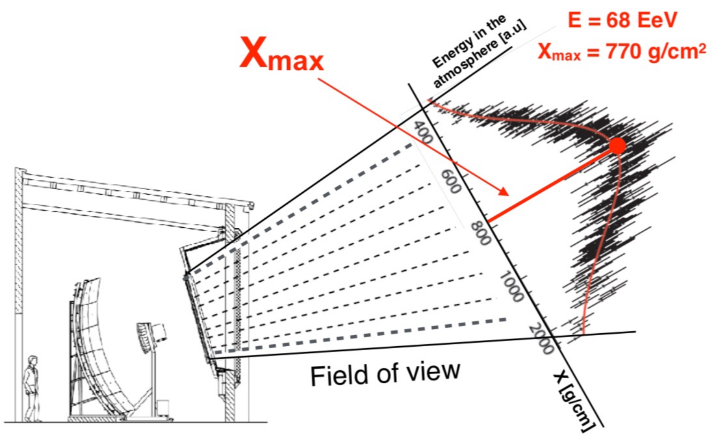

Measurement of the primary CR energy with the FD

A shower detected by the SD and by the FD, reconstructed with zenith angle θ = 36.3° and energy *E* = 16.76 EeV.

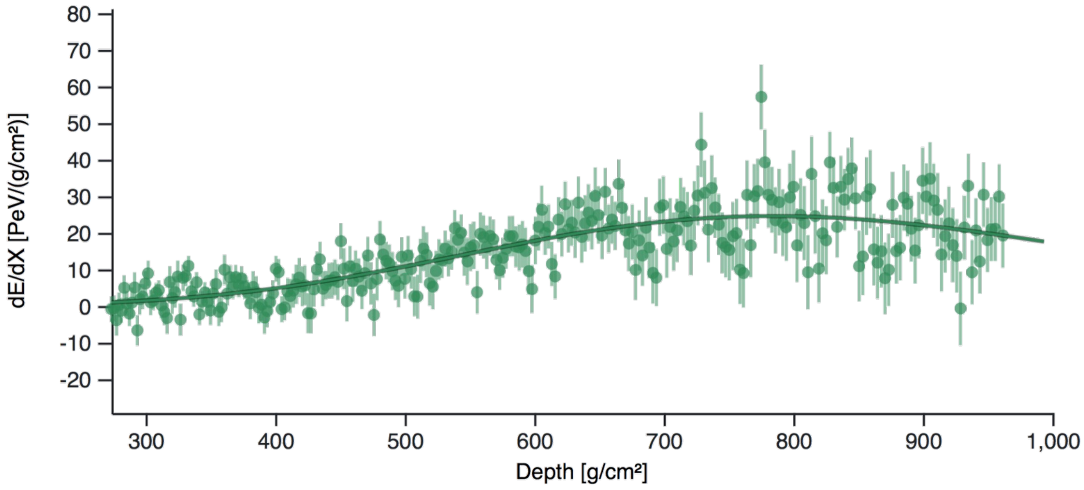

Energy deposited in the atmosphere per unit length vs. the **<u>slant depth</u>** crossed by the cosmic ray.

The **integral** of this curve gives an **estimate of the energy**

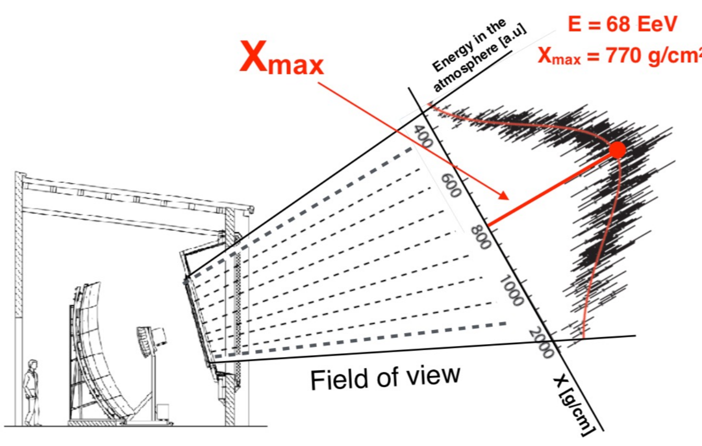

Longitudinal profile for a high elevation shower

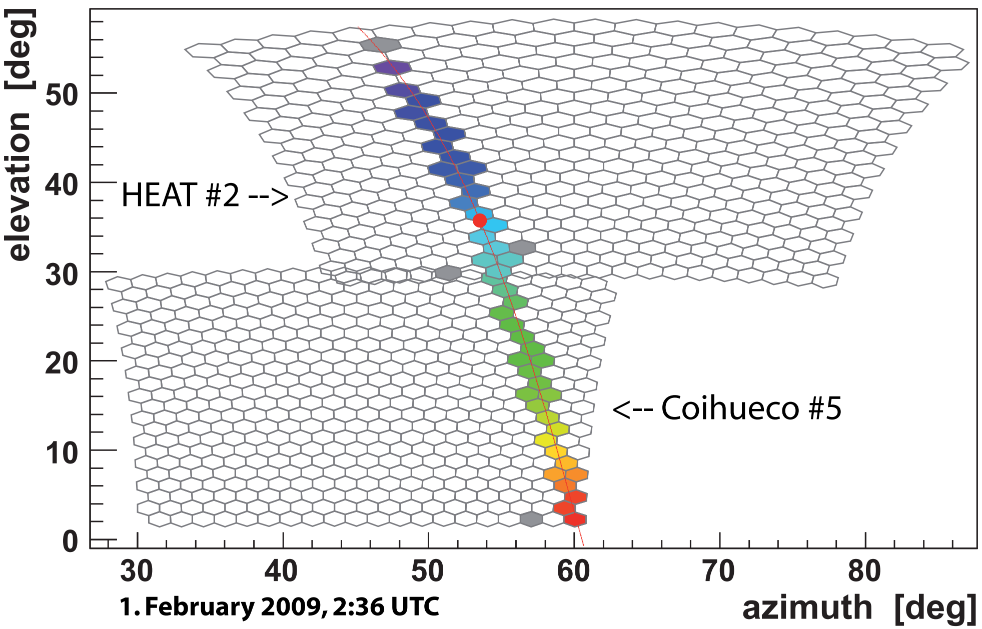

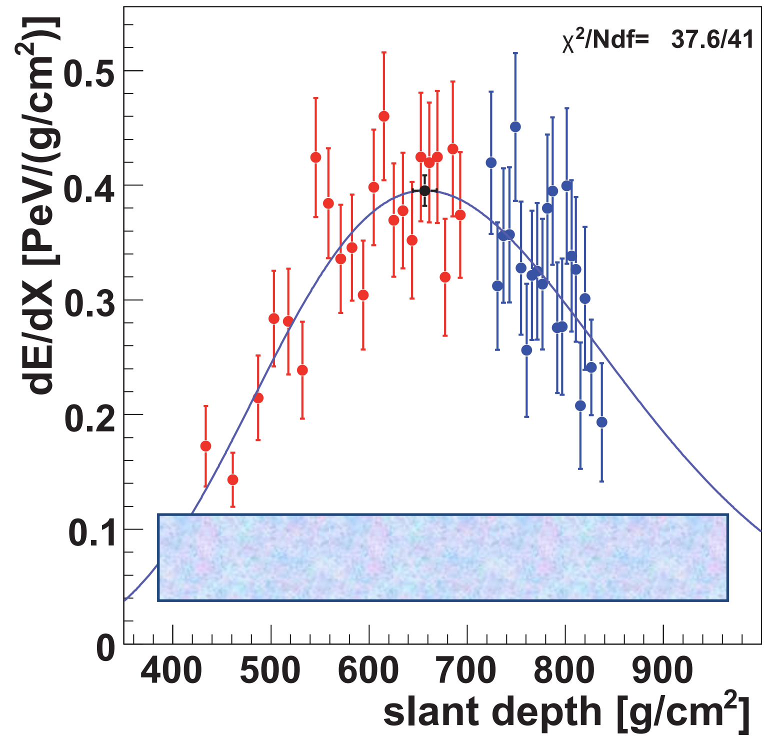

Which is the correct legend?

● (red) HEAT	● (blue) HEAT
● (blue) Coihueco	● (red) Coihueco

Longitudinal profile for a high elevation shower

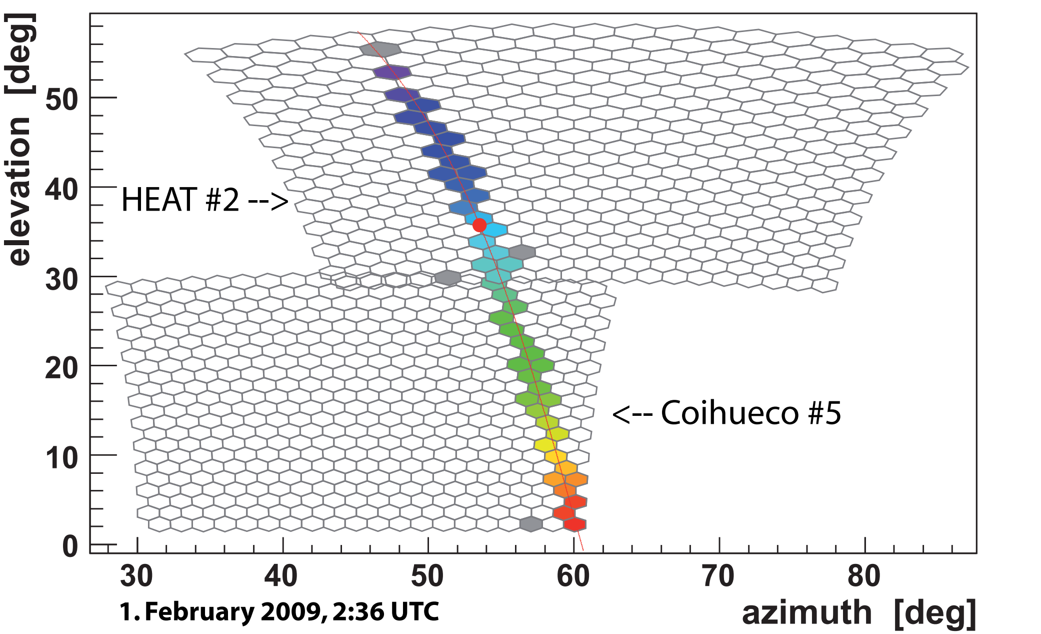

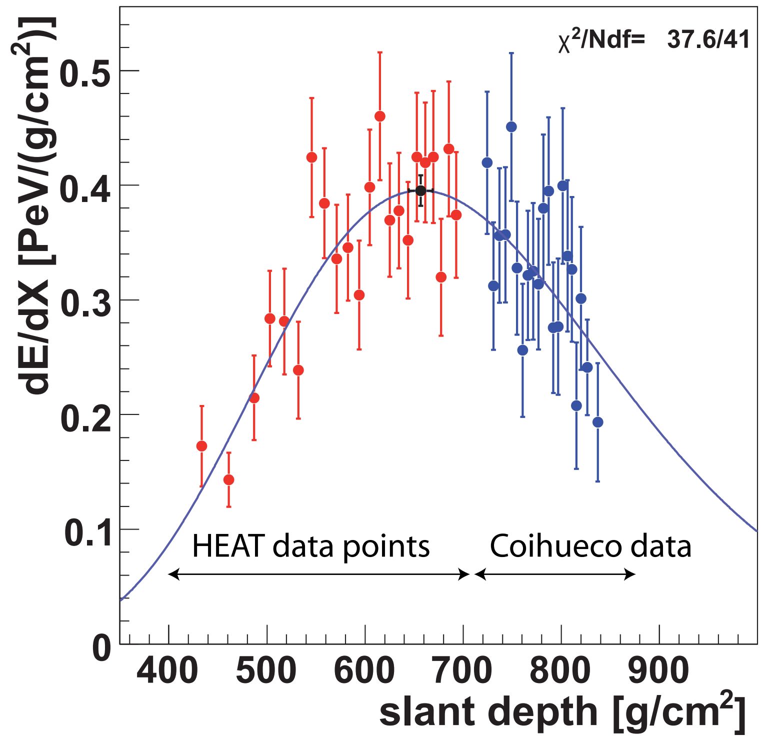

HEAT

Coihueco

Relative error on the energy estimate

[Auger Collaboration, PHYSICAL REVIEW D 102, 062005 (2020)]

Error bars: stat. uncertainties on the point
Shaded band: stat. uncertainties on the fit

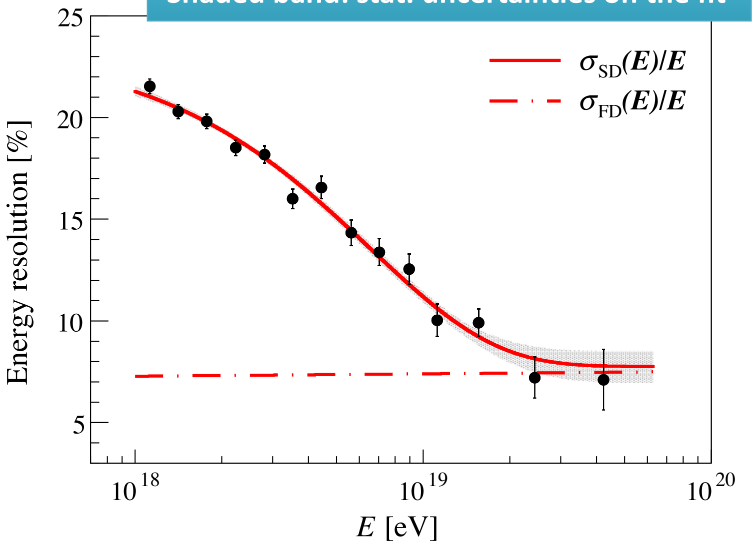

- The relative error on the energy estimated with the **FD (dotted-dashed red line)** is :

$$\frac{\sigma_{\mathrm{FD}}(E)}{E} \cong 7.4\%$$

- The relative error on the energy estimated with the **SD (continuous red line)** is well described with the fit function:

$$\frac{\sigma_{\mathrm{SD}}(E)}{E} = \sigma_0 + \sigma_1 \exp\left(-\frac{E}{E_\sigma}\right)$$

Differential energy flux above 2.5×10^{18} eV

[Auger Collaboration, PHYSICAL REVIEW D 102, 062005 (2020)]

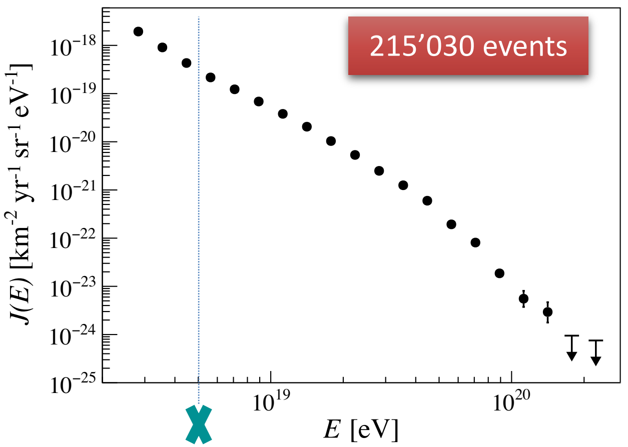

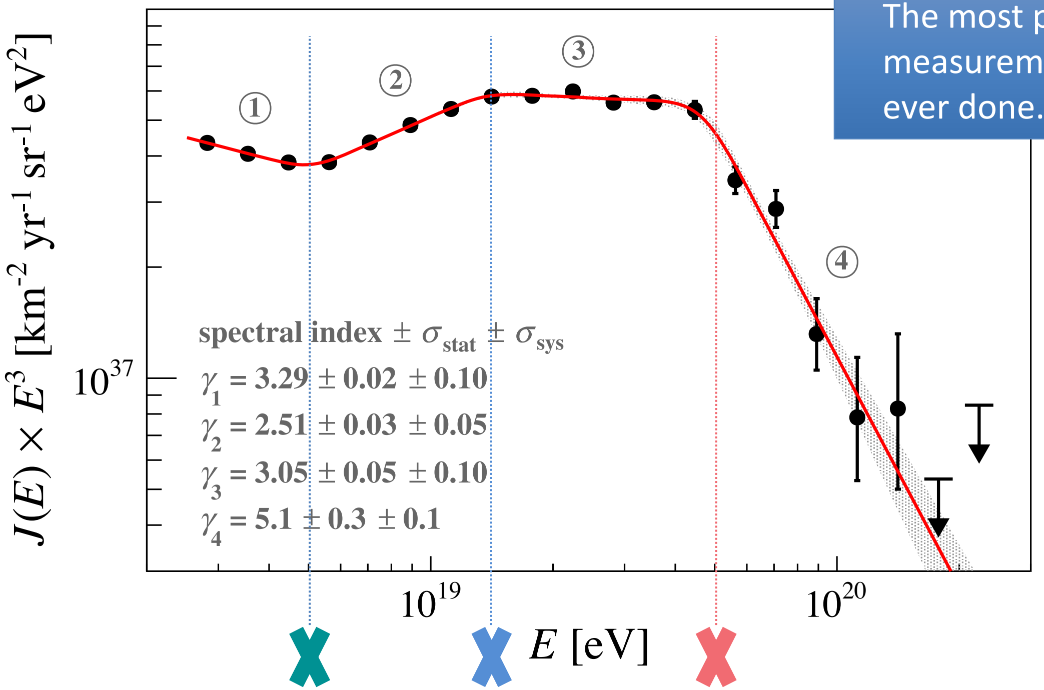

The most precise measurement ever done.

1. The so-called **«ankle»** of the spectrum, near 5×10^{18} eV, is confirmed.
2. A new feature has been identified in the spectrum: above the «ankle» the spectral index **changes from γ_2 to γ_3**.
3. The **steepening of the spectrum at around 5×10^{19} eV** is confirmed.

End of the CR spectrum

Energy spectrum suppression above ~ 5 x 10^{19} eV confirmed unambiguously

[Auger Collaboration, JCAP04(2017)038]

1^{st} Hp: protons dominate at the highest energies

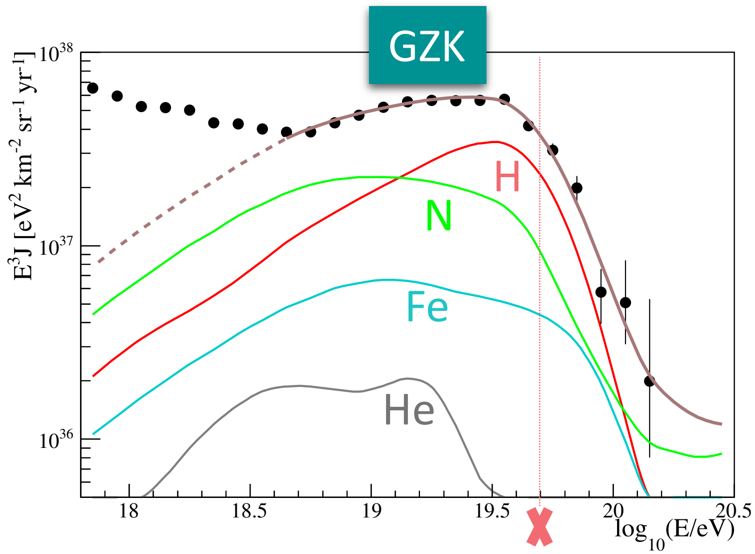

Propagation effect

Energy spectrum suppression due to the GZK effect

2^{nd} Hp: Heavier nuclei dominate at the highest energies

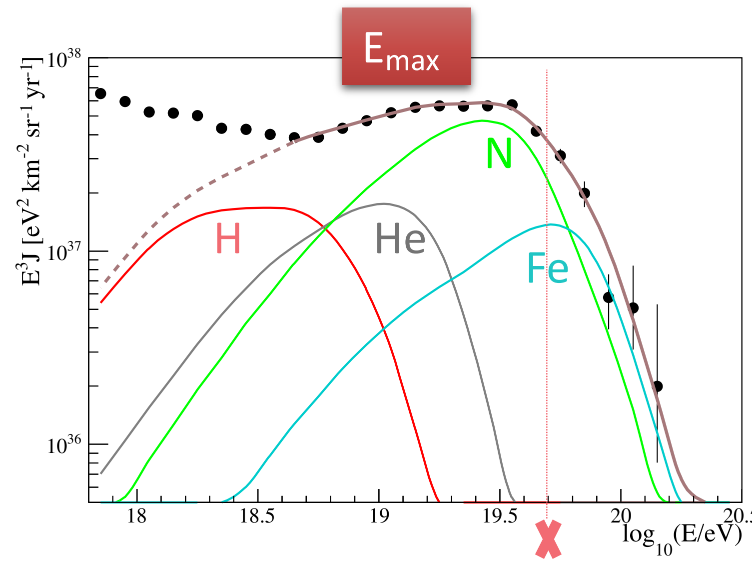

Source effect

Energy spectrum suppression due to the maximum acceleration energy

$E_{max}(A) = Z\, E_{max}(p)$

(sources run out of steam)

What is the origin of the spectrum suppression? E_{max} or GZK?

Reconstruction of the primary CR mass with the FD

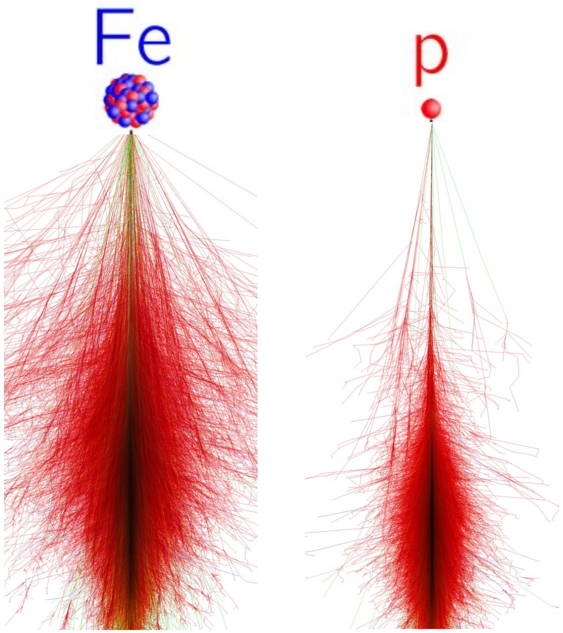

$X_{max}(Fe) < X_{max}(p)$

$\sigma[X_{max}(Fe)] < \sigma[X_{max}(p)]$

The depth at which the maximum of the energy deposition occurs (***X*max**) is used to infer the **primary particle mass**.

The Pierre Auger Observatory and its Upgrade

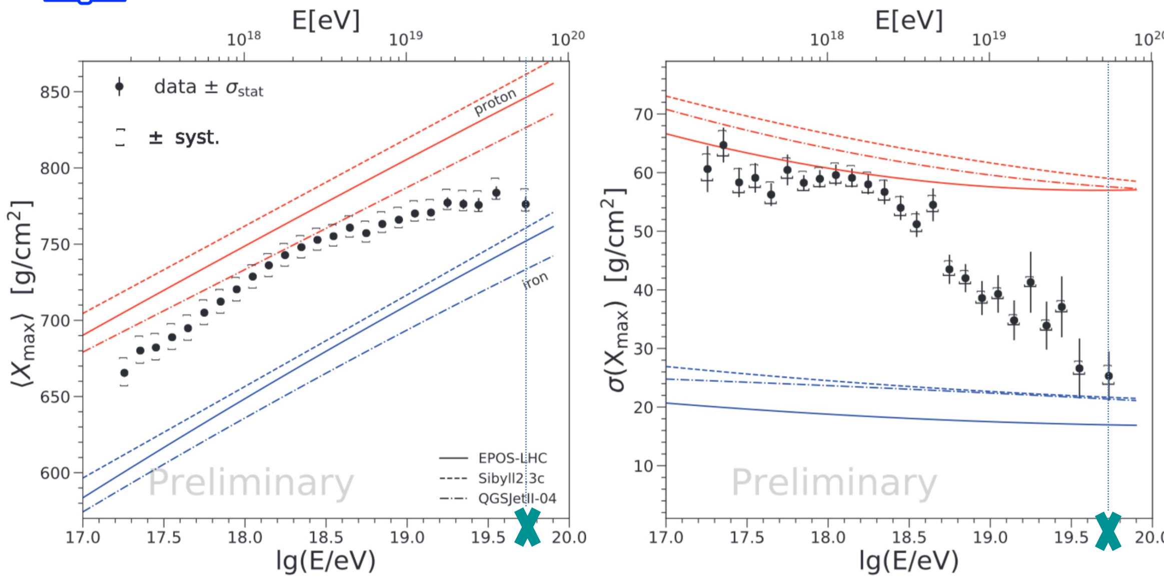

- Mass composition NOT constant:
  - At low energy: composition compatible with a light or mixed one;
  - At high energy: composition quite heavy.
- The inferred mass composition relies heavily on the hadronic interaction models.

Muonic component

The muonic component derives from the decay of charged pions and kaons.

Since muons do not multiply and lose their energy only by ionization, the muon component after its maximum attenuates slowly, differently from the electronic component which disappears rapidly.

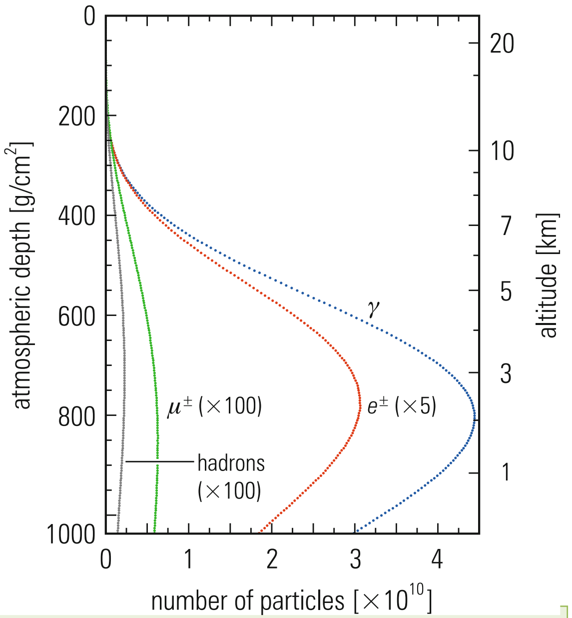

From Monte Carlo simulations:

$$(N_\mu)_p \propto E_0^{0.86}$$

Total number of muons with energy > 1 GeV in a shower produced by a **proton** of energy E_0.

$$(N_\mu)_A \propto A^{0.14}\,(N_\mu)_p$$

Total number of muons with energy > 1 GeV in a shower produced by a **nucleus of mass number *A*** and energy E_0.

Showers from light primaries contain less muons

E_{max} or GZK?

Increasing the statistics with the currently working detectors is not sufficient, we need:

1. measurement of the primary CR mass with SD at the highest energies **&**
2. measurement of the shower muon component

The future of Auger: Auger Prime

[The Pierre Auger Observatory and its Upgrade]

1. **New Scintillator Surface Detector (SSD):** primarily sensitive to the e.m. component of the EAS. Combined with the SD, which responds to both e.m. particles and muons, it enables an improved estimation of the muon content.
2. Upgrade of the Underground Muon Detector (UMD).
   [**Showers from light primaries contain less muons**]

- New **Radio Detector (RD)** on each water Cherenkov station (3000 km^2 radio array) → measurement of the radio emission of air showers.
- **Increase of the FD operation time** (extend measurements into periods with higher night sky background and twilight) by reducing the PMT gain from 50 k to 5 k → **FD enables direct measurements of X_{max} - currently the best method of mass composition determination.**
- **SD electronics improvements**:
  - faster sampling of ADC traces
  - better GPS timing accuracy
  - larger dynamic range
  - more sophisticated local triggers.

The upgrade of the Pierre Auger Observatory is ongoing.
Operation of the upgraded Observatory is expected for at least 10 years.

Neutral cosmic rays: cosmic photons

Astronomy

Up to a couple of decades ago, our knowledge of the Universe was mainly based on observations of electromagnetic radiations of different wavelengths.

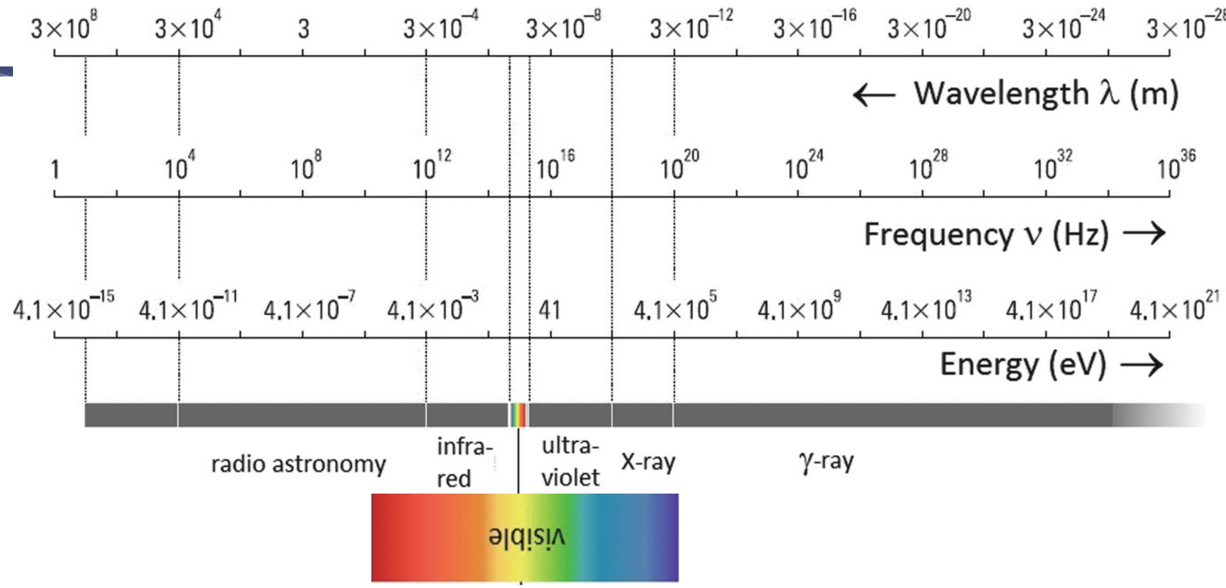

- **Astronomy** (i.e., the identification of cosmic sources in the sky) is only possible with neutral probes (photons and neutrinos) of any energy and with very high-energy protons.
  - ✓ **Charged particles at very high energies (>10^{19} eV) travel along approximately straight lines through the** irregular interstellar and intergalactic magnetic fields.

➢ Gravitational Waves

Detection of cosmic photons

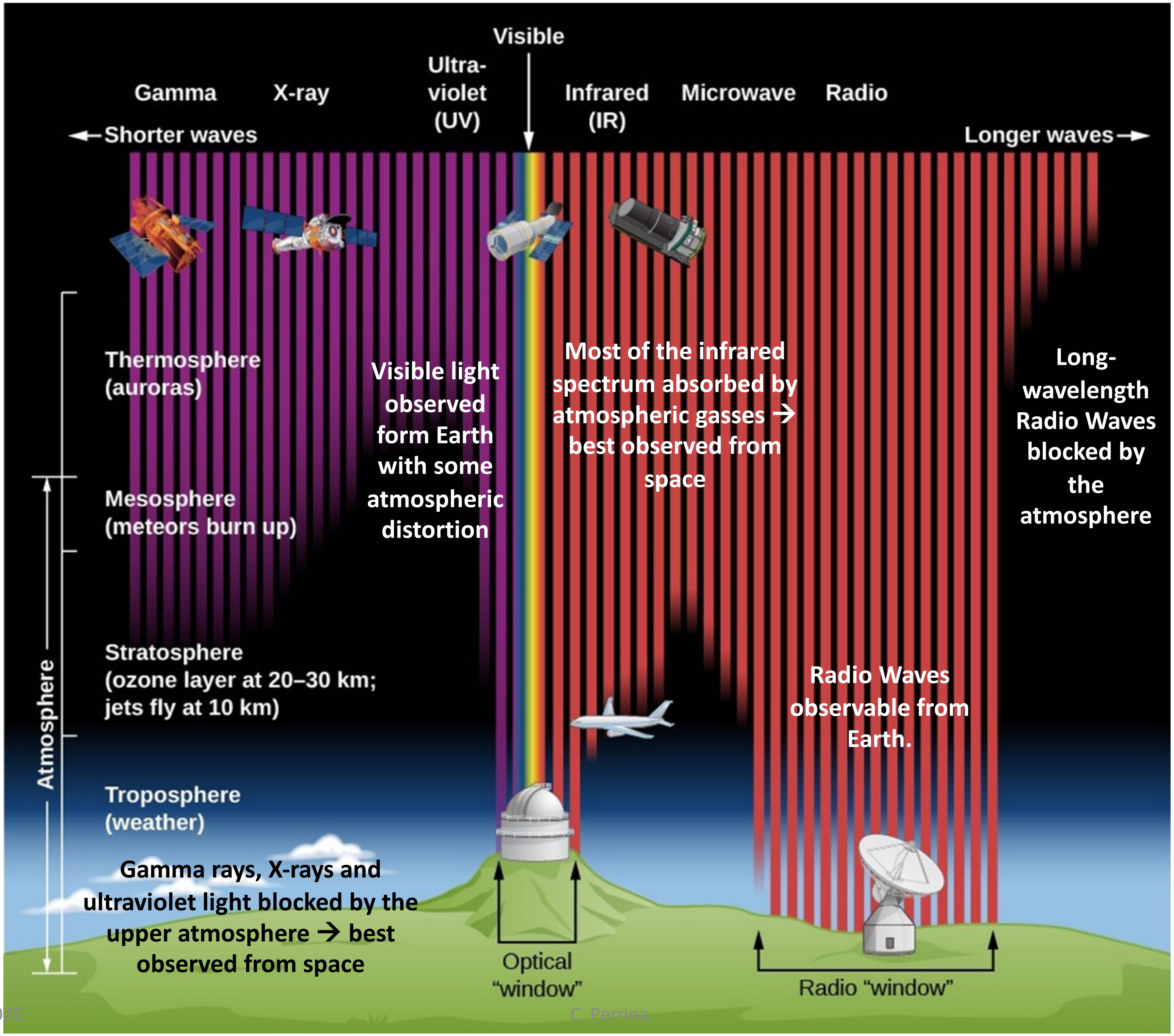

Sources of Gamma Rays (10 MeV – 100 TeV)

https://glast.sites.stanford.edu/fermi-overview-presentation

Photon Production mechanisms

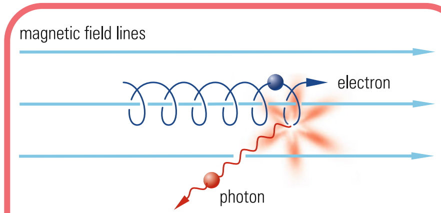

Synchrotron radiation

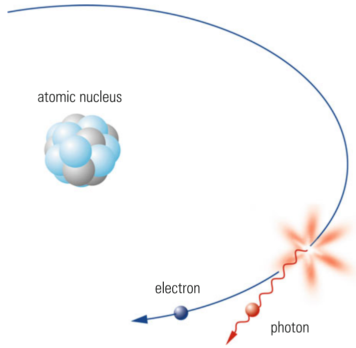

Bremsstrahlung

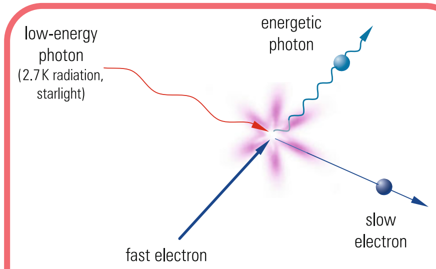

Inverse Compton Scattering

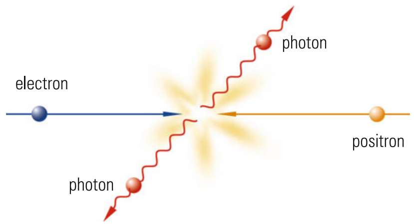

Matter–Antimatter Annihilation

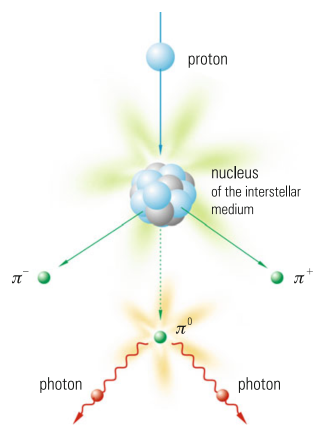

Decay of π^0

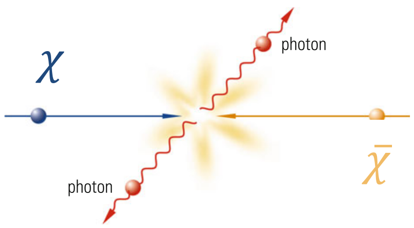

DM–DM Annihilation

$$^{60}\mathrm{Co} \rightarrow {}^{60}\mathrm{Ni}^{**} + e^- + \bar{\nu}_e$$
$$\hookrightarrow {}^{60}\mathrm{Ni}^{*} + \gamma(1.17\,\mathrm{MeV})$$
$$\hookrightarrow {}^{60}\mathrm{Ni} + \gamma(1.33\,\mathrm{MeV})\,.$$

Nuclear Transformations

Spectral Energy Distribution (SED)

$F(\nu)$ «**Spectral flux density**»: the rate at which energy is transferred by electromagnetic radiation through a real or virtual surface, per unit area and unit frequency ν.
Possible units are erg s^{-1} cm^{-2} Hz^{-1}

$$J(\nu) \propto \nu F(\nu) = E_\gamma^2 \frac{dN_\gamma}{dE_\gamma}$$

«**Flux density**» , it is used to compare the electromagnetic energy emission in different region of the electromagnetic spectrum. Possible units are erg s^{-1} cm^{-2}

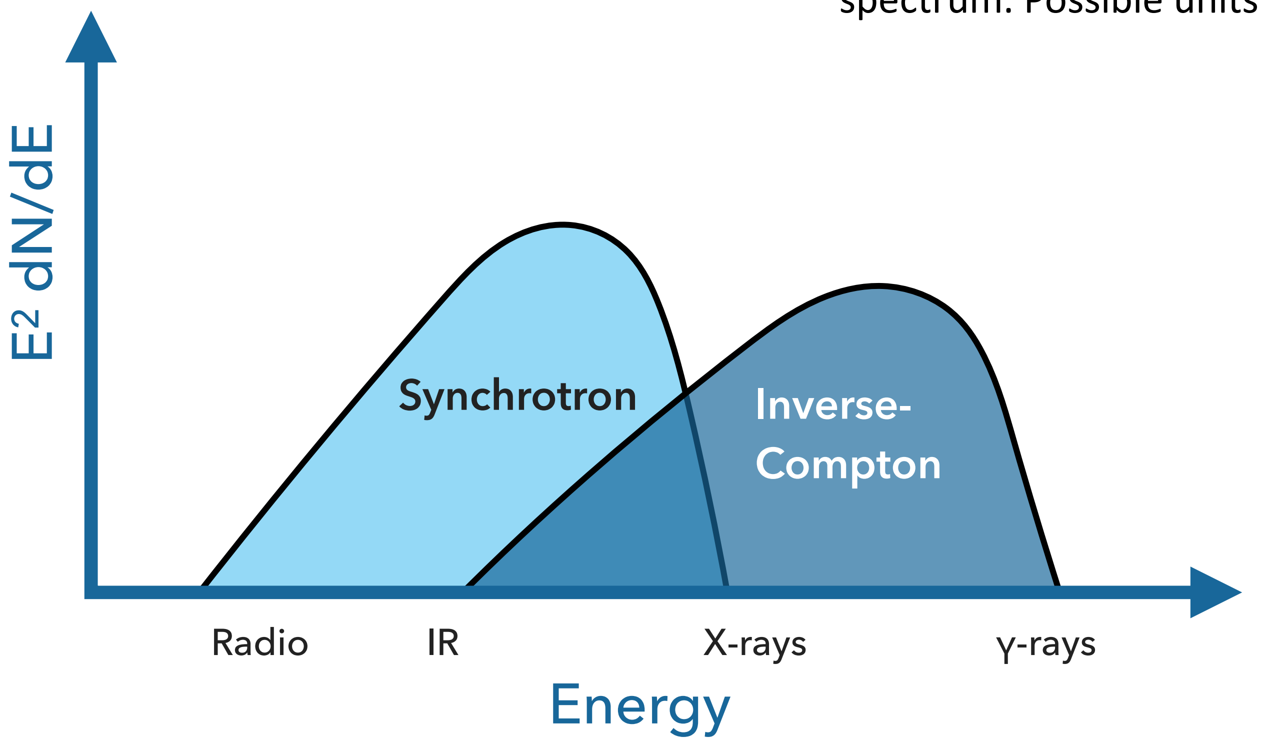

Spectral Energy Distribution (SED)

Inverse Compton → Leptonic Production

Pion Bump → Hadronic Production

????

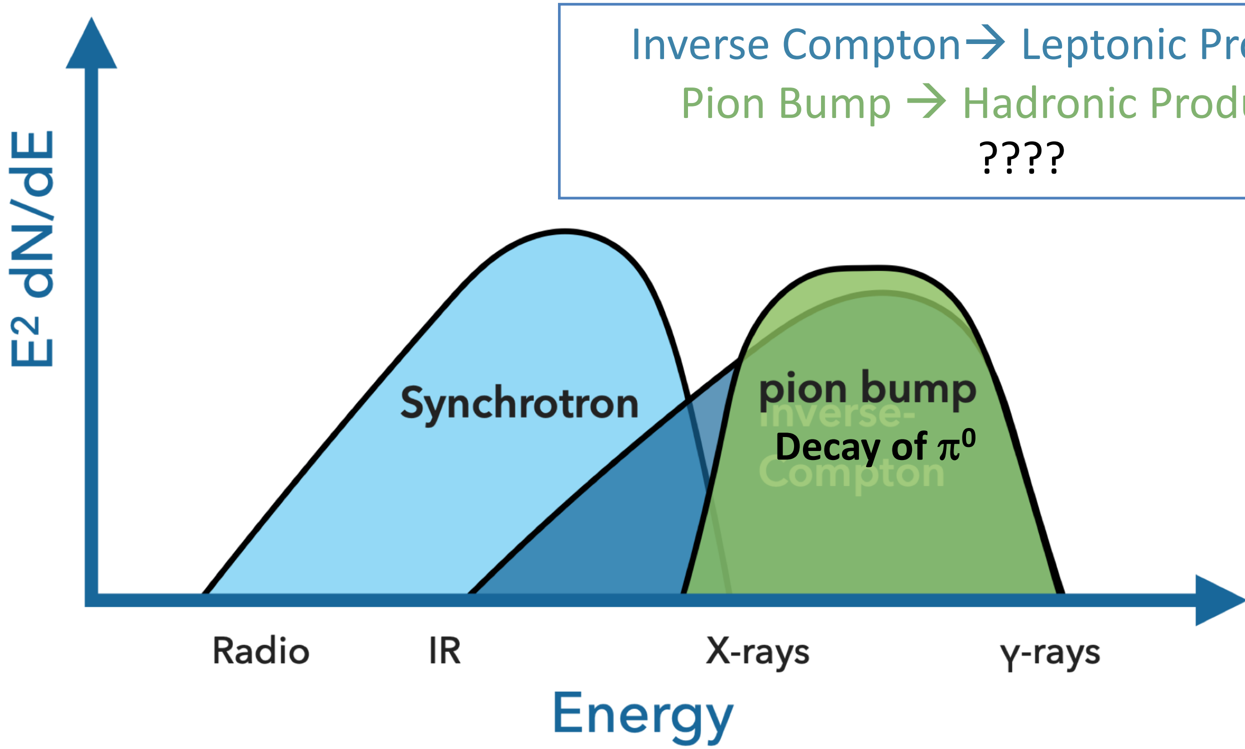

SED measurements

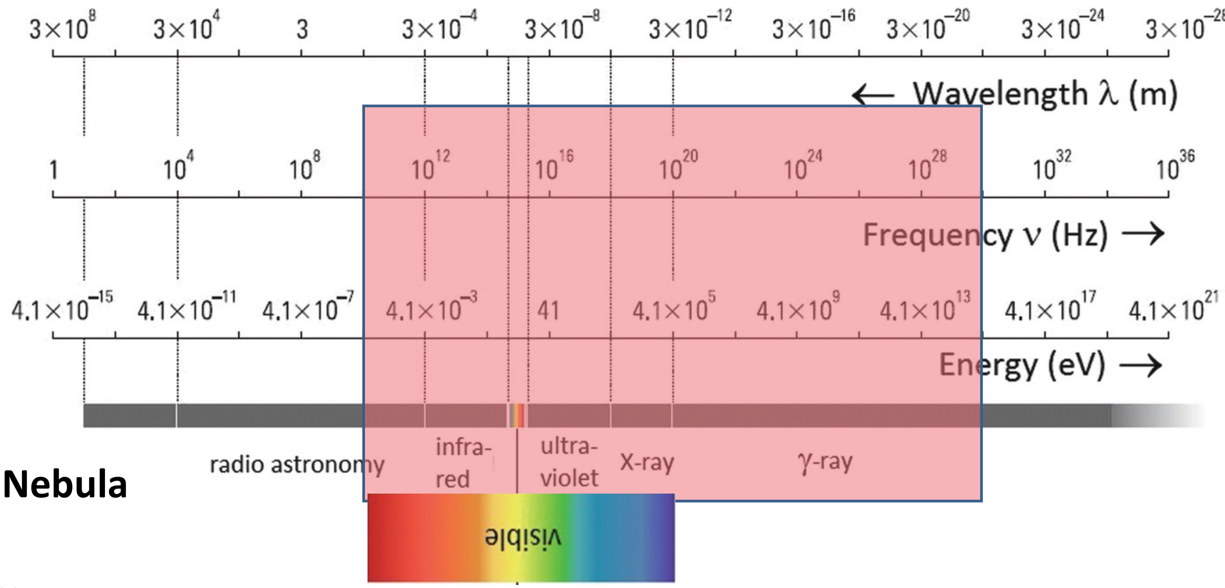

Integral flux density of the Crab Nebula

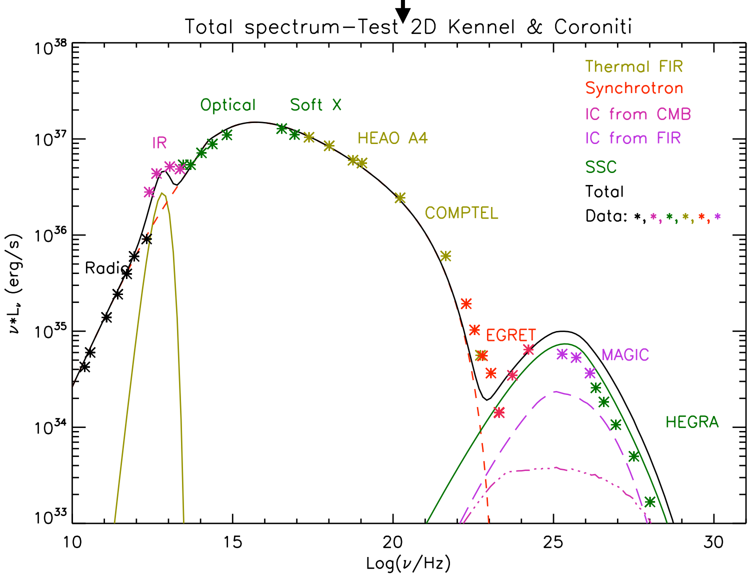

D. Volpi et al., AIP Conference Proceedings 983, 216 (2008)

Pulsar Wind Nebulae (e.g., Vela and Crab Nebula) are characterized by non-thermal radiation at all wavelengths, mostly synchrotron (from radio to X-ray bands) and Inverse Compton (gamma-ray band),

SSC: Synchrotron Self-Compton, is the process occurring when high-energy electrons emit synchrotron radiation and then they inverse scatter the produced synchrotron photons increasing their energy.
FIR: Far Infrared Radiation

Gamma-ray experiments (now)

Satellites (*E* < 100 GeV)

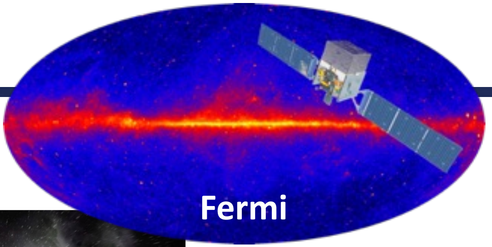

Imaging Atmospheric Cherenkov Telescopes “IACTs” (*E* > 100 GeV)

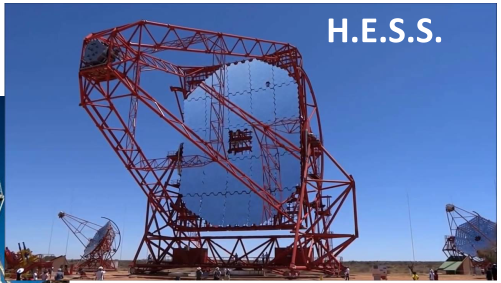

Extensive Air Shower Detectors (*E* < 100 TeV)

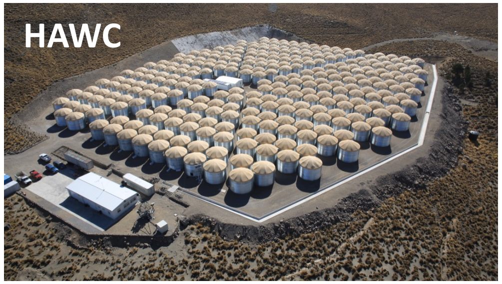

Fermi (2008 -- now)

Formerly called the **Gamma-ray Large Area Space Telescope** (**GLAST**).
Also called Fermi Gamma-Ray Space Telescope (FGST).

- Launched on June 11, 2008.
- **Fermi** is a satellite experiment for the observation of the cosmos. Fermi **studies the extreme phenomena of the universe**, from gamma-ray bursts and black-hole jets to pulsars and supernova remnants.

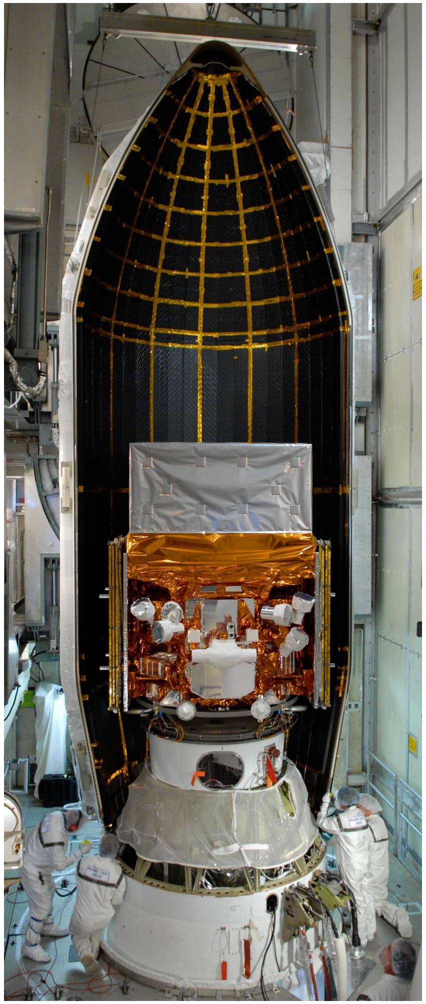

5-10 years (planned), still running (~ 17 years)

https://www.nasa.gov/content/fermi-gamma-ray-space-telescope
Live orbit: https://www.n2yo.com/?s=33053

Fermi Collaboration (12 Countries)

Country	Funding Agencies
United States	NASA; Department of Energy
France	Commissariat à l'Energie Atomique; CNRS/Institut National de Physique Nucléaire et de Physique des Particules
Italy	Agenzia Spaziale Italiana; Istituto Nazionale di Fisica Nucleare; Istituto Nazionale di Astrofisica
Japan	Ministry of Education, Culture, Sports, Science and Technology; High Energy Accelerator Research Organization (KEK); Japan Aerospace Exploration Agency
Sweden	K. A. Wallenberg Foundation; Swedish Research Council; National Space Board

Non funding countries: Germany, Iceland, Ireland, Slovenia, South Africa, Spain, United Kingdom

Fermi detectors and sky coverage

4.3 tons (DAMPE: 1.45 tons)
$1.8 \times 1.8 \times 2.8\ \mathrm{m}^3$ (DAMPE: $1.2 \times 1.2 \times 1\ \mathrm{m}^3$)

Large Area Telescope (LAT)

- **16 identical towers (4 x 4 matrix)**

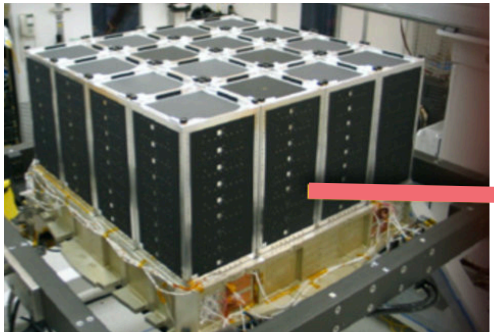

Gamma-ray Burst Monitor (GBM)

- **14 scintillator detectors**

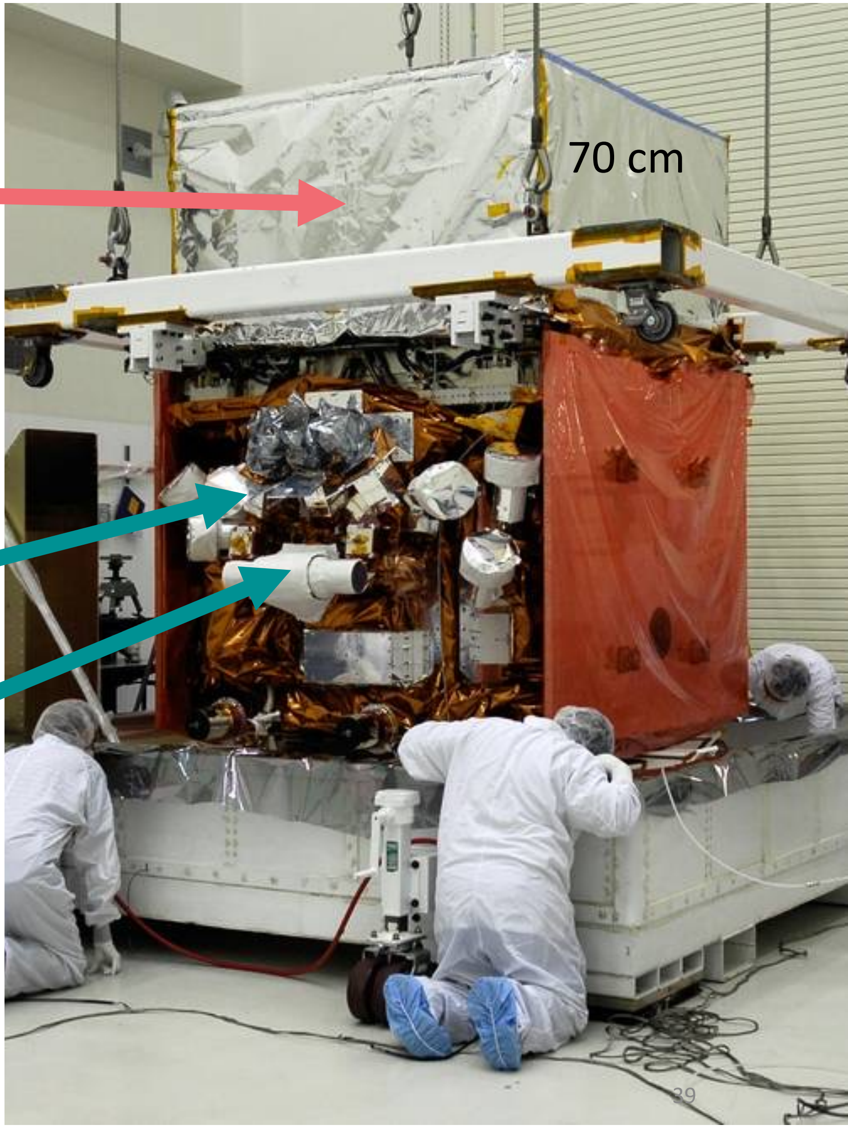

Fermi detectors: LAT and GBM

Large Area Telescope (LAT)

- **16 identical towers**
- **Each tower is a pair-conversion telescope with a calorimeter**
    - Background rejection: 99.9999%.
    - Angular resolution: 0.1°
    - Energy range: 20 MeV to > 300 GeV

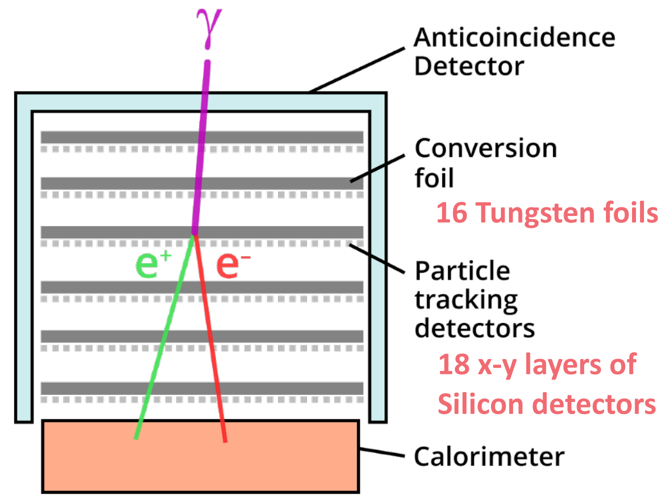

https://www.youtube.com/watch?v=ESkHDCEAqZk

NaI (location & low-energy spectrum)

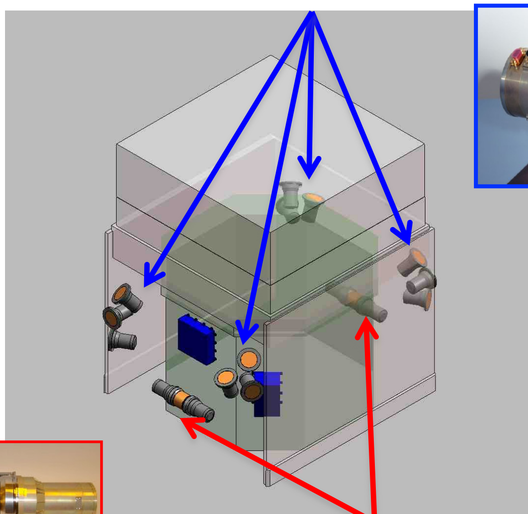

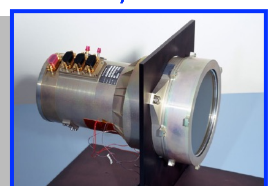

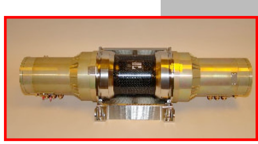

BGOs (mid-energy spectrum)

Gamma-ray Burst Monitor (GBM)

- **12 Sodium Iodide (NaI) scintillators**
    - Energy range: 8 keV to 1 MeV
    - Burst trigger and location within few degrees
- **2 Bismuth Germanate (BGO) scintillators**
    - Energy range: 150 keV to 30 MeV

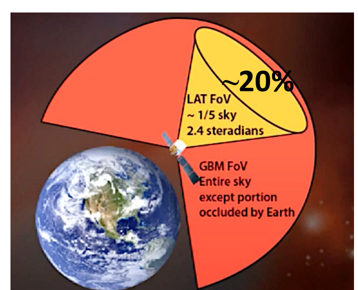

→ complete sweep of the sky every ~3 hours
https://fermi.gsfc.nasa.gov/ssc/observations/types/post_anomaly/

LAT visibility

The orbital period is **96.5 minutes**.
LAT can scan the full sky in 2 orbits (~ 3 hours).

Galactic Latitude (symbol *b*) measures the angle of an object northward of the galactic equator.

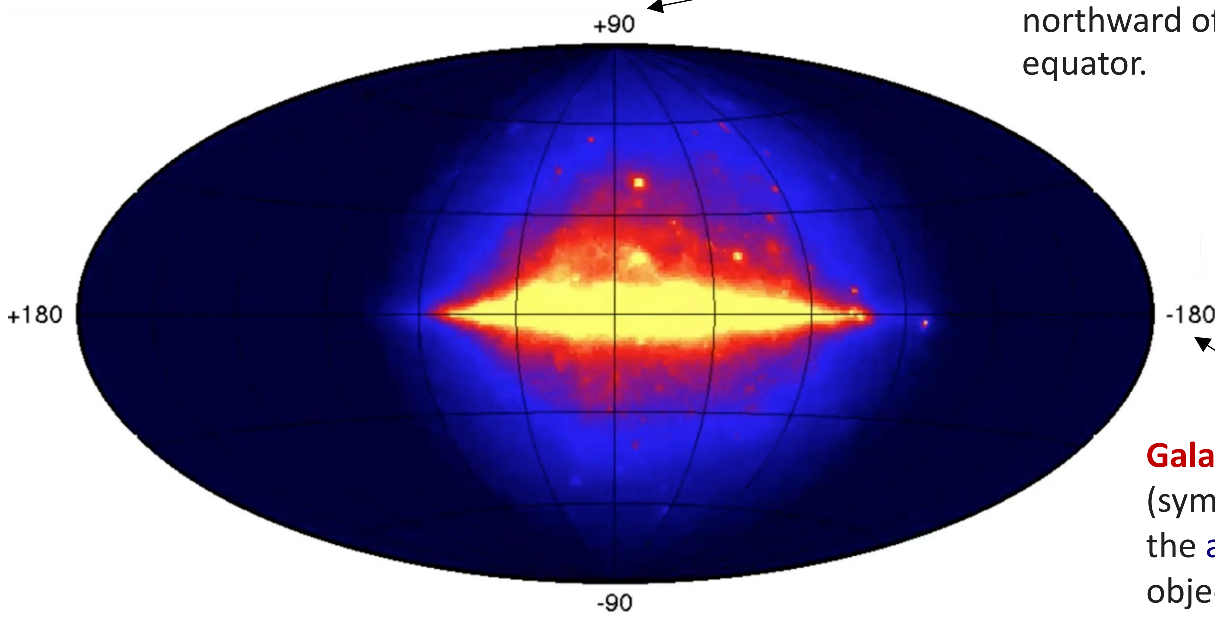

Galactic Longitude (symbol *l*) measures the angular distance of an object eastward along the galactic equator from the galactic center.

https://fermi.gsfc.nasa.gov/ssc/data/access/lat/LightCurveRepository/

Extraordinary features of GBM

- GBM detects more than 200 gamma ray bursts (GRBs) per year.
- GBM detects a GRB → the spacecraft can orient LAT in the GRB direction.
- GBM transmits the burst data to ground stations which then forward Fermi's information to the **Swift** telescope and **other multiwavelength observers** for detailed analysis of the GRB source (https://www.astronomerstelegram.org. The Astronomer's Telegram (ATel) is an available online database of astronomical research and discoveries of transient sources. A ATel entry usually includes the name, coordinates, and event type, as well as more detailed information, such as its frequency band, spectral and temporal evolution, and the results of follow-up observations. ATels are typically released within hours or days after an observation and provide a quick overview of the discovery and initial analysis.

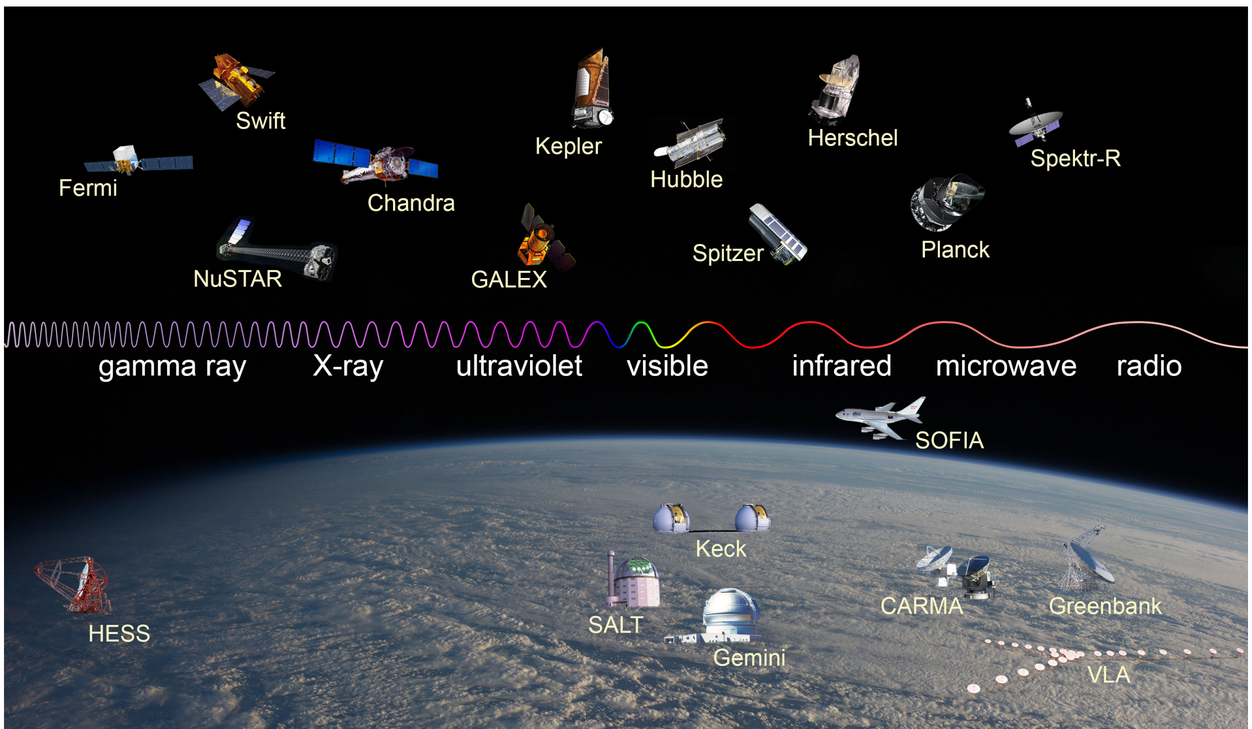

Fermi science program

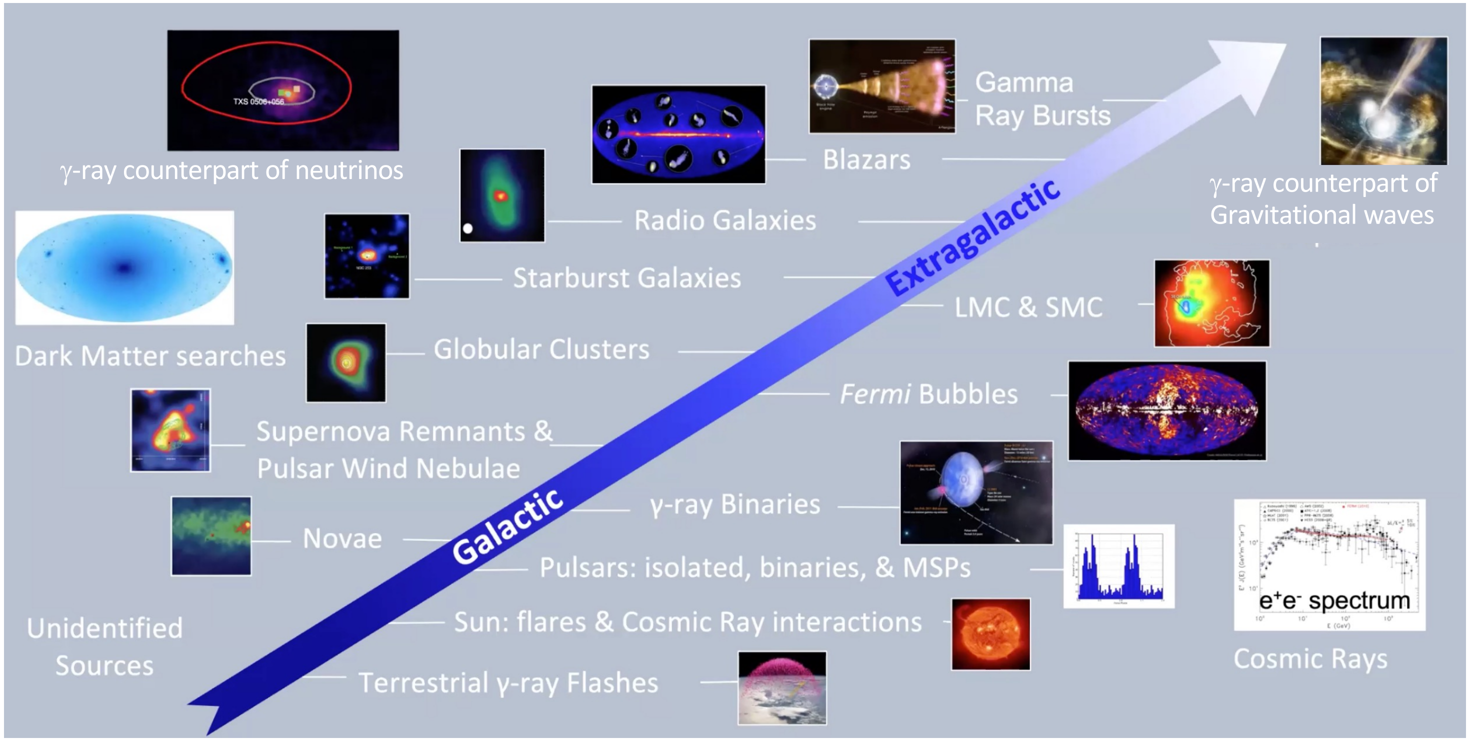

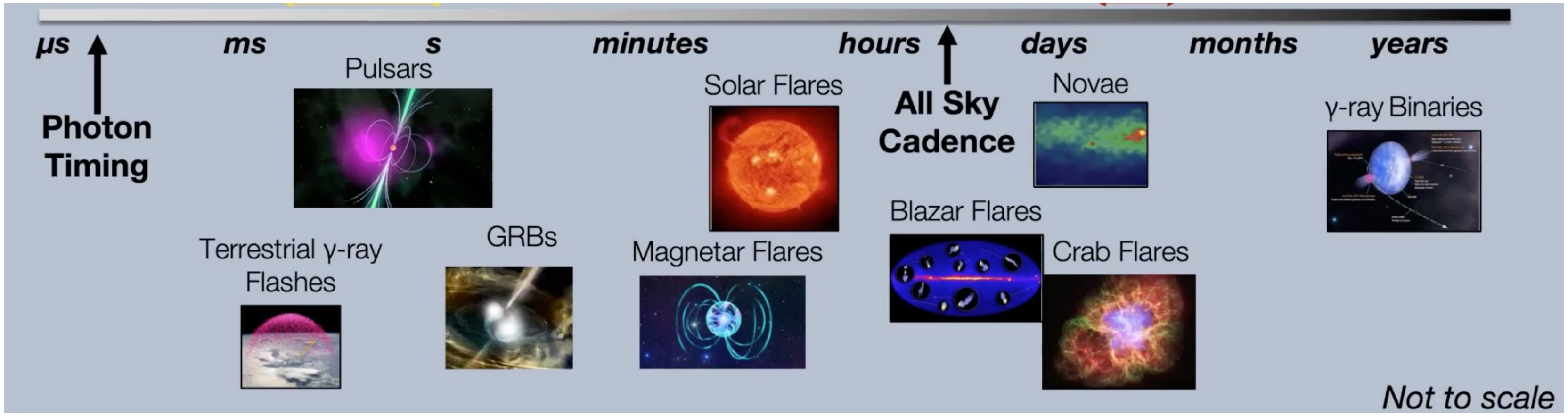

All-Sky Map

Data taken by the Energetic Gamma Ray Experiment Telescope (EGRET) aboard the Compton Gamma Ray Observatory (CGRO), using 9 years of data,from 1991 to 2000

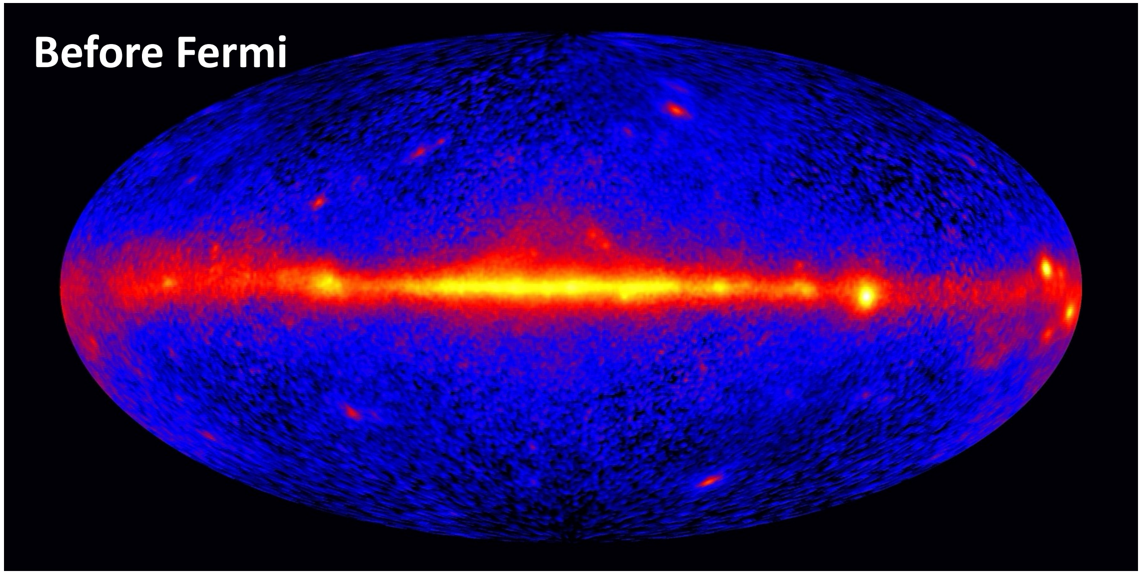

Data taken by Fermi using 9 years of data collected from 2008 to 2017.

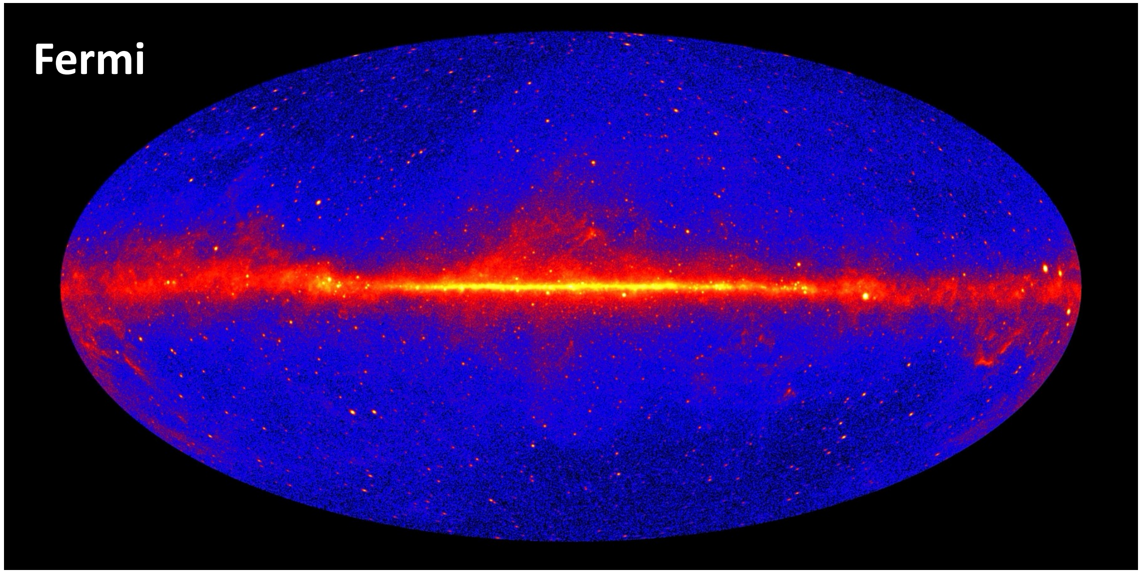

DAMPE All-Sky Map

DAMPE can scan the full sky in 6 months.

- Selected events in galactic coordinates for 8 years of flight data (2016-2023) with $E_{rec} \in [1, 10^4]$ GeV

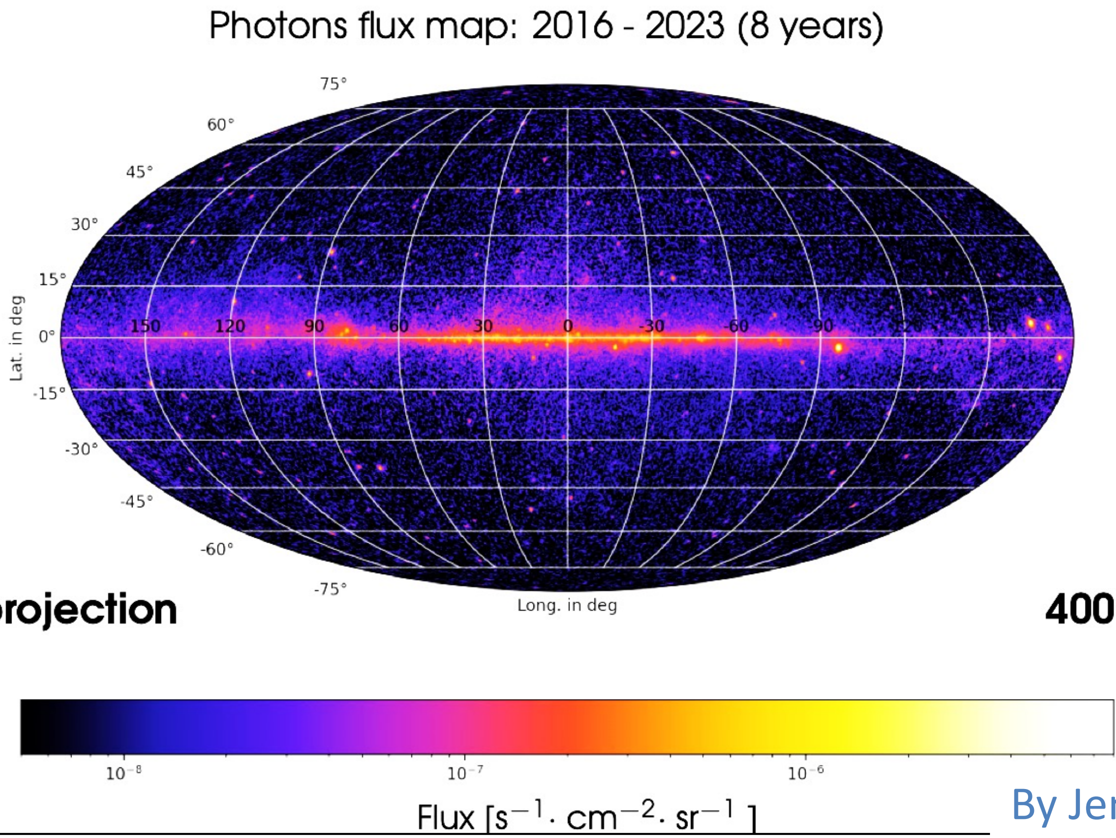

Mollweide projection

400’303 events

By Jennifer Frieden (PhD student, EPFL)

Fermi LAT 4th Catalog

S. Abdollahi et al 2020 ApJS **247** 33

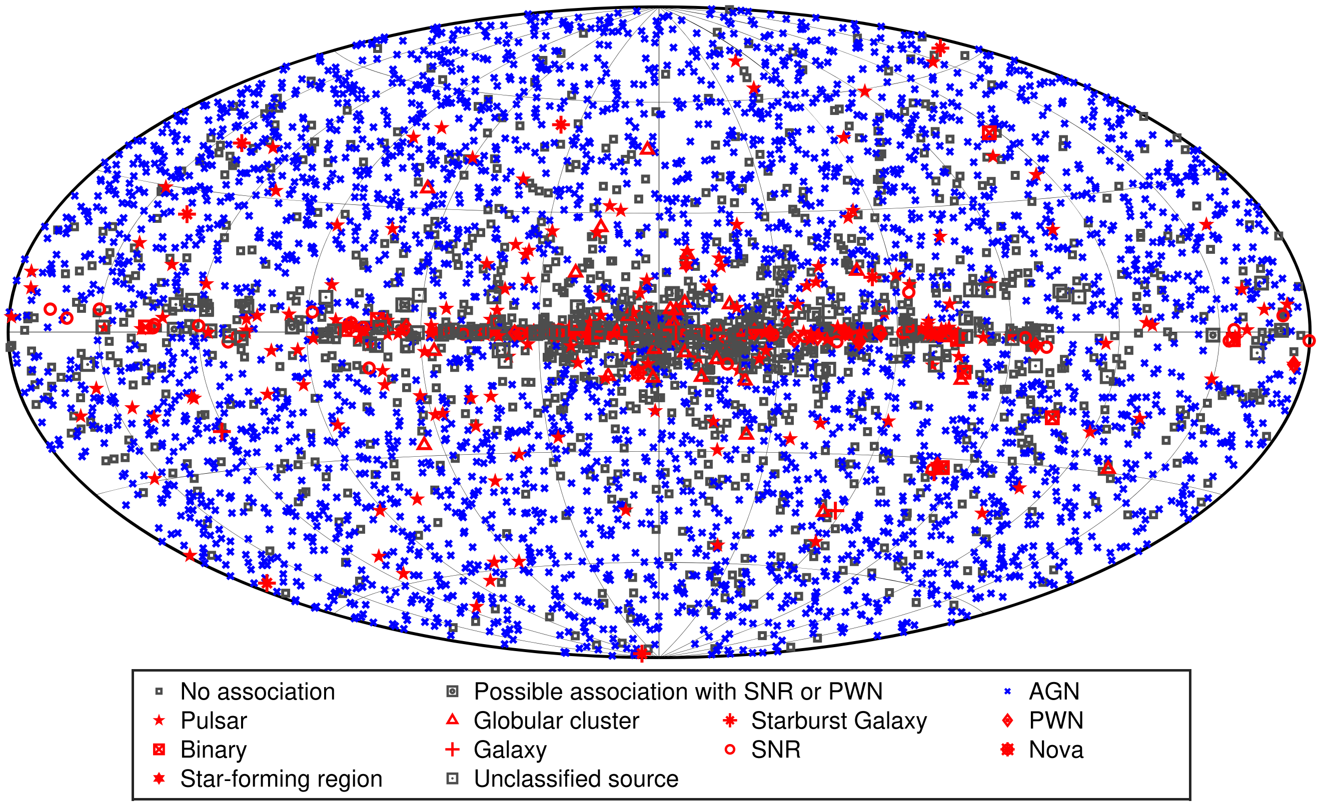

Fermi LAT 4th Catalog

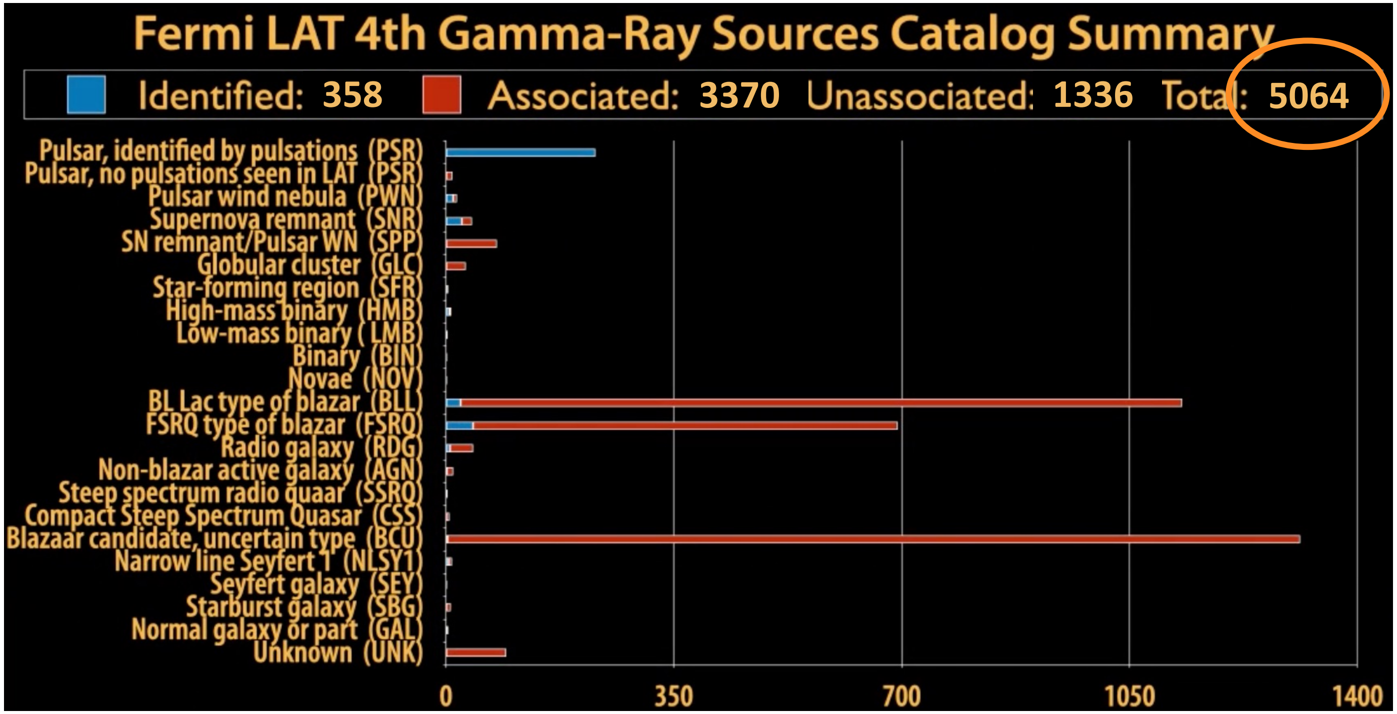

The 4FGL catalog includes 5064 sources above 4σ significance, for which localization and spectral properties are provided.

- **358 sources** are considered as **identified** based on angular extent, periodicity, or correlated variability observed at other wavelengths.
  - **239 are pulsars**.
- **> 3130 of the identified or associated** sources are active galaxies of the **blazar** class.
- 1336 sources have not counterparts at other wavelengths (unassociated).

Detection of GRB 090510 – Lorentz Invariance validation

C. Couturier et al., https://arxiv.org/pdf/1308.6403.pdf

The Lorentz Invariance prediction of Einstein's Special Theory of Relativity hold that all observers measure the same speed of light in vacuum i.e., the speed of light in vacuum does not depend on the energy of photons.

In May 2009, both low energy (30 MeV) and high energy (30 GeV) photons from a GRB were detected by Fermi at the same time.

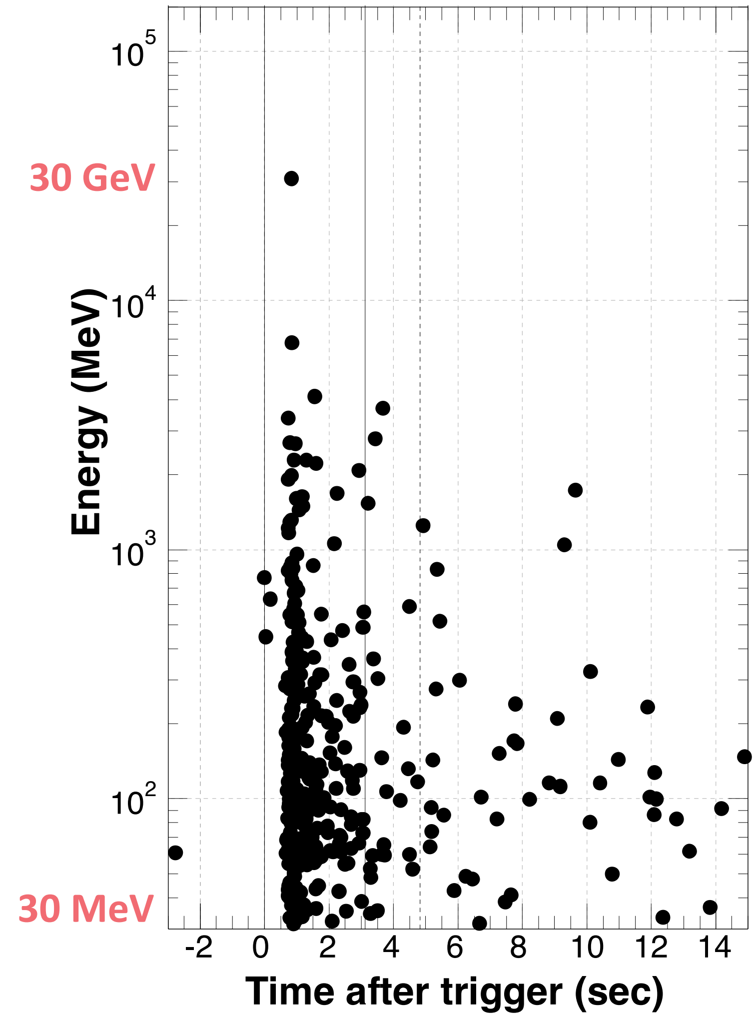

Fermi and LIGO detect a Binary Neutron Star Merger

- At 8:41 a.m. EST on August 17, 2017, **LIGO,** the twin **L**aser **I**nterferometer **G**ravitational Wave **O**bservatories in Hanford (WA, USA) and Livingston (LA, USA) detected a **gravitational wave** signal.

- The VIRGO interferometer near Pisa (Italy) detected the same signal.

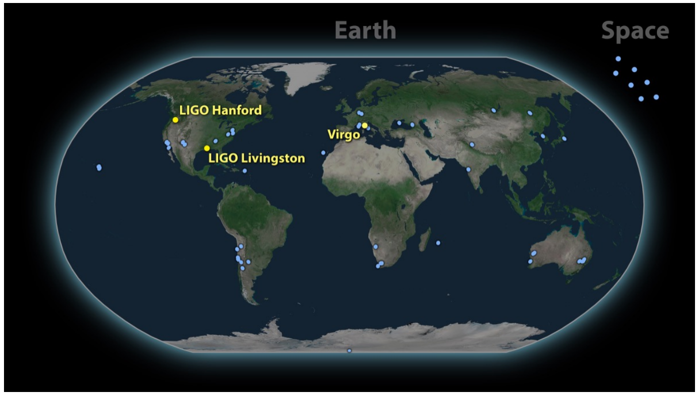

This Gravitational wave signal had the theoretical predicted characteristic of a binary neutron star merger from the galaxy NGC 4993 that should produce a **very short high energy gamma ray burst**.

- 2 s later, the Fermi GBM detected a very short, high energy GRB in the galaxy NGC 4993, located 130 million light-years from the Earth in the constellation Hydra.

- LIGO/VIRGO and Fermi sent worldwide a notification that triggered more than 70 follow-up detections and confirmations of this **multimessenger** event.

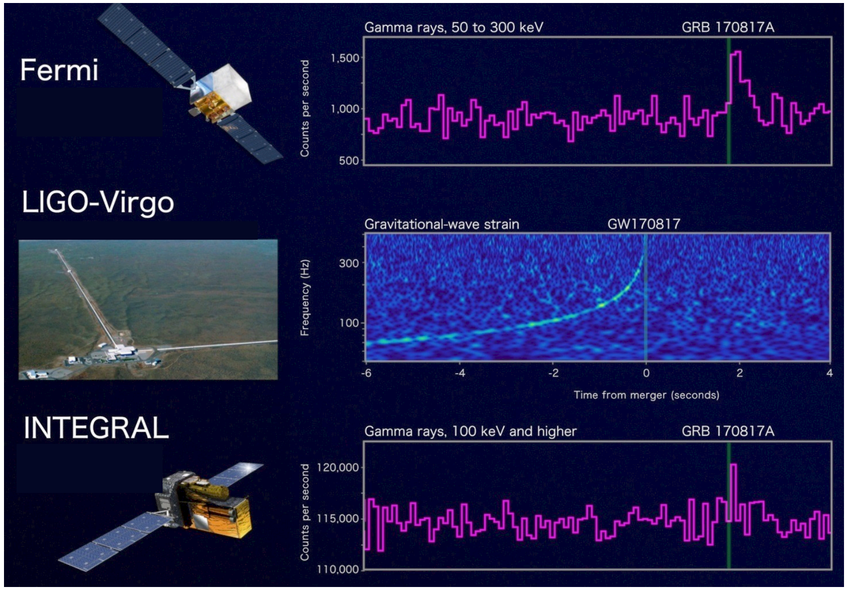

Lesson 4 -- Bibliography

- **Probes of Multimessenger Astrophysics** Chapter 4 and Chapter 7

  Maurizio Spurio

  Springer (Second Edition)

  https://link.springer.com/book/10.1007%2F978-3-319-96854-4

- **The Review of Particle Physics (2022)**

- **Introduction to Particle and Astroparticle Physics** Chapter 4.5.3: Detection of Hard Photons

  Alessandro De Angelis and Mário Pimenta

  Springer (Second Edition, 2018)

  https://link.springer.com/book/10.1007%2F978-3-319-78181-5

- **Auger publications:**

  https://www.auger.org/index.php/science/journal-articles

- **Telescope Array publications:**

  http://www.telescopearray.org/index.php/research/publications/journal-publications